

THE UNIVERSITY OF CALGARY

THE CHEMICAL AND STABLE ISOTOPIC
CHARACTERIZATION OF SULPHATE
CONTAMINATED GROUNDWATER NEAR A SOUR
GAS PLANT

by

Catrin van Donkelaar

A THESIS

SUBMITTED TO THE FACULTY OF GRADUATE STUDIES
IN PARTIAL FULFILLMENT OF THE REQUIREMENTS FOR THE
DEGREE OF MASTER OF SCIENCE

DEPARTMENT OF GEOLOGY AND GEOPHYSICS

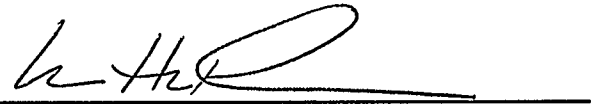
CALGARY, ALBERTA

NOVEMBER, 1993

© Catrin van Donkelaar 1993

THE UNIVERSITY OF CALGARY
FACULTY OF GRADUATE STUDIES

The undersigned certify that they have read, and recommend to the Faculty of Graduate Studies for acceptance, a thesis entitled "The Chemical and Stable Isotopic Characterization of Sulphate Contaminated Groundwater Near a Sour Gas Plant" submitted by Catrin van Donkelaar in partial fulfillment of the requirements for the degree of Master of Science.



Supervisor, Dr. Ian E. Hutcheon,
Department of Geology & Geophysics



Dr. L.R. Bentley,
Department of Geology & Geophysics



Dr. H. Roy Krouse,
Department of Physics and Astronomy

December 4, 1993

Abstract

The objectives for this thesis are to assess $\delta^{34}\text{S}$ as a tracer of anthropogenic sulphate in groundwater and to document geochemical interactions that take place as a result of industrial sulphate loading. During four separate sampling excursions, groundwater samples were obtained from 13 piezometers which surround the elemental sulphur storage blocks at an Alberta sour gas plant. Each sample was analyzed for $\delta^{34}\text{S}_{\text{sulphate}}$, $\delta^{18}\text{O}_{\text{sulphate}}$, $\delta^{18}\text{O}_{\text{water}}$, δD , major aqueous species, alkalinity, pH, temperature and dissolved oxygen. Hydraulic head measurements were taken to define the groundwater flow field. In the study area, anthropogenic sulphate has a $\delta^{34}\text{S}$ of approximately +18‰ (CDT), while natural groundwater sulphate is depleted to about -12‰. $\delta^{34}\text{S}$ is a conservative tracer at this site. Groundwater sulphate concentrations increase as $\delta^{34}\text{S}$ approaches +18‰, suggesting that elevated sulphate concentrations are due to sulphur released by sour gas processing. Acidic waters generated by the gas plant are neutralized by rock-water reactions.

Acknowledgements

I am grateful to: my supervisor Ian Hutcheon for his wisdom and contagious humour, Dr. Krouse for introducing me to the wonders of stable isotopes, and Larry Bentley for helping me explain my groundwater mysteries. I am also thankful for funding from Shell Canada Ltd. and NSERC.

My grasp of stable isotopes was enhanced by discussions with Dr. Bernard Mayer and fellow graduate students Ann-Lise Norman and Mike Weiser. I would also like to thank the chefs of the stable isotope lab: Jesusa, Nenita and Maria for helping me with my isotope analyses and force feeding me.

Thanks to the Dudes of Diagenesis (Graham, J. Cody, George, Stevo, Cindy, Maurice, Arthur, Scott's) for the laughs and advice. Thank you to Pat Micheal for my cations, XRF and general assistance and Deb Glatiotis for the XRD work. Also, thanks to Dr. H. Abercrombie and Brad Gorman at the I.S.P.G. for anion analyses.

I also want to thank John Fennell and KOMEX International Ltd. for assistance with field sampling and lively groundwater discussions. I can't divulge the name of my secret study site but I want to thank Norris Graham and Kim Johnson, their support was essential for this thesis.

Finally, thank you Paul, the man who rubs my back.

Table of Contents

Approval Page.....	ii
Abstract.....	iii
Acknowledgements.....	iv
Table of Contents	v
List of Tables.....	vii
List of Figures.....	viii
Epigraph.....	ix
CHAPTER 1: BACKGROUND	
1.1 Introduction.....	1
1.2 Past Work.....	4
1.3 Thesis Objectives	5
1.4 Methods	
1.40 Field Methods.....	7
1.41 Field Sample Preservation	9
1.42 Laboratory.....	10
CHAPTER 2: SETTING	
2.1 Climate	15
2.2 Topography	15
2.3 Geology.....	18
2.4 Hydrogeology.....	21
CHAPTER 3: GEOCHEMICAL AND ISOTOPIC DATA, OBSERVATIONS AND TRENDS	
3.1 Ionic Strengths	30
3.2 Sulphate Concentrations.....	32
3.3 Calcium, Magnesium and Sodium Concentrations.....	36
3.4 Stable Isotopes.....	40
CHAPTER 4: $\delta^{34}\text{S}$ AS A TRACER OF ANTHROPOGENIC SULPHATE IN SHALLOW GROUNDWATER	
4.1 Sulphate Reducing Bacteria	44
4.2 Anthropogenic Sulphate Identified with $\delta^{34}\text{S}$	48

**CHAPTER 5: ALTERATION OF GROUNDWATER CHEMISTRY
BY SULPHATE**

5.1 Introduction of Sulphuric Acid.....55
5.2 Geochemical Evidence of Acid Buffering by Minerals in
Glacial Till55
5.3 Isotopic Evidence of Ancient Carbonates in Glacial Tills as an
Acid Buffer.....60
5.4 Gypsum Precipitation in Sulphate Contaminated
Groundwater.....63

CHAPTER 6: CONCLUSIONS.....71

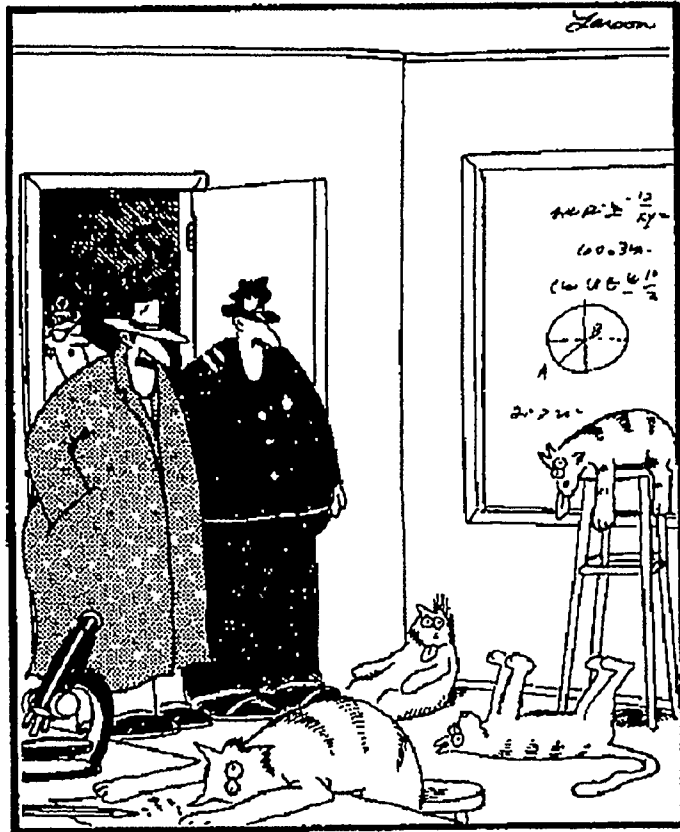
REFERENCES.....73

List of Tables

TABLE 1	Summary of data acquired and rationale	8
TABLE 2	Chemical and isotope data summary.....	14
TABLE 3	Hydrogeology data summary.....	23
TABLE 4	$\delta^{34}\text{S}$ of incubated November 1992 samples.....	48
TABLE 5	Soil investigation data summary	69

List of Figures

Figure 1.1	sulphate loading cartoon.....	1
Figure 1.2	piezometer schematic.....	9
Figure 2.1	bar chart of monthly precipitation.....	16
Figure 2.2	study area and site topography.....	17
Figure 2.3	drill cutting logs	19
Figure 2.4	groundwater movement cartoon.....	21
Figure 2.5	bar chart of hydraulic head variation.....	24
Figure 2.6	hydraulic head contour map.....	25
Figure 3.1	bar chart of ionic strengths.....	31
Figure 3.2	ionic strength as a function of $[\text{SO}_4^{2-}]$	32
Figure 3.3	plot of $[\text{Ca}^{2+}]$ and $[\text{Mg}^{2+}]$ versus $[\text{SO}_4^{2-}]$	33
Figure 3.4	$[\text{SO}_4^{2-}]$ contamination plume near piezometer7	35
Figure 3.5	stick diagram of $[\text{Ca}^{2+}]$ concentrations	37
Figure 3.6	stick diagram of $[\text{Mg}^{2+}]$ concentrations.....	38
Figure 3.7	plot of $[\text{Ca}^{2+}]$ versus $[\text{Na}^+]$ from piezometer 13S	39
Figure 3.8	$\delta^{34}\text{S}$ as a function of ionic strength	41
Figure 3.9	$\delta^{34}\text{S}$ as a function of $[\text{SO}_4^{2-}]$	42
Figure 4.1	$\delta^{18}\text{O}_{\text{sulphate}}$ versus $\delta^{34}\text{S}$	45
Figure 4.2	distribution of $\delta^{34}\text{S}$ values.....	49
Figure 4.3	downward movement of ^{34}S rich contaminant plume	50
Figure 4.4	$\delta^{34}\text{S}$ as a function of vertical gradient, 7B to 7C.....	51
Figure 4.5	$\delta^{34}\text{S}$ as a function of vertical gradient, 4B to 4C.....	52
Figure 4.6	plot of $\delta^{34}\text{S}$ versus $[\text{SO}_4^{2-}]^{-1}$	54
Figure 5.1	plot of $[\text{Ca}^{2+}]$ versus $[\text{SO}_4^{2-}]$	56
Figure 5.2	plot of alkalinity versus $[\text{SO}_4^{2-}]$	58
Figure 5.3	$[\text{Ca}^{2+}]$, $[\text{Mg}^{2+}]$ activity Mg-Ca Beidellite equilibrium.....	59
Figure 5.4	δD versus $\delta^{18}\text{O}$, ^{18}O enrichment relative to MWL.....	60
Figure 5.5	plot of $\delta^{18}\text{O}$ increases with $[\text{Ca}^{2+}]$	61
Figure 5.6	plot of $\delta^{18}\text{O}$ increases with alkalinity.....	62
Figure 5.7	gypsum saturation indices increasing with $\delta^{34}\text{S}$	66
Figure 5.8	cross-section of data from soil investigation	70



"Notice all the computations, theoretical scribbles, and lab equipment, Norm. ... Yes, curiosity killed these cats."

The Far Side©. FARWORKS INC. distributed by Universal Press Syndicate.
reprinted with permission. all rights reserved.

CHAPTER 1: BACKGROUND

1.1 Introduction

Since the early 1900's, sour (H_2S containing) gas plants in Alberta have been introducing industrial sulphur into the natural environment mainly as sulphur dioxide emissions. In addition, stock-piled elemental sulphur can be transported off-site as wind borne particulates, with surface runoff, and/or by leaching into the groundwater system. The principal mechanisms by which sulphate enters groundwater are illustrated in Figure 1.1.

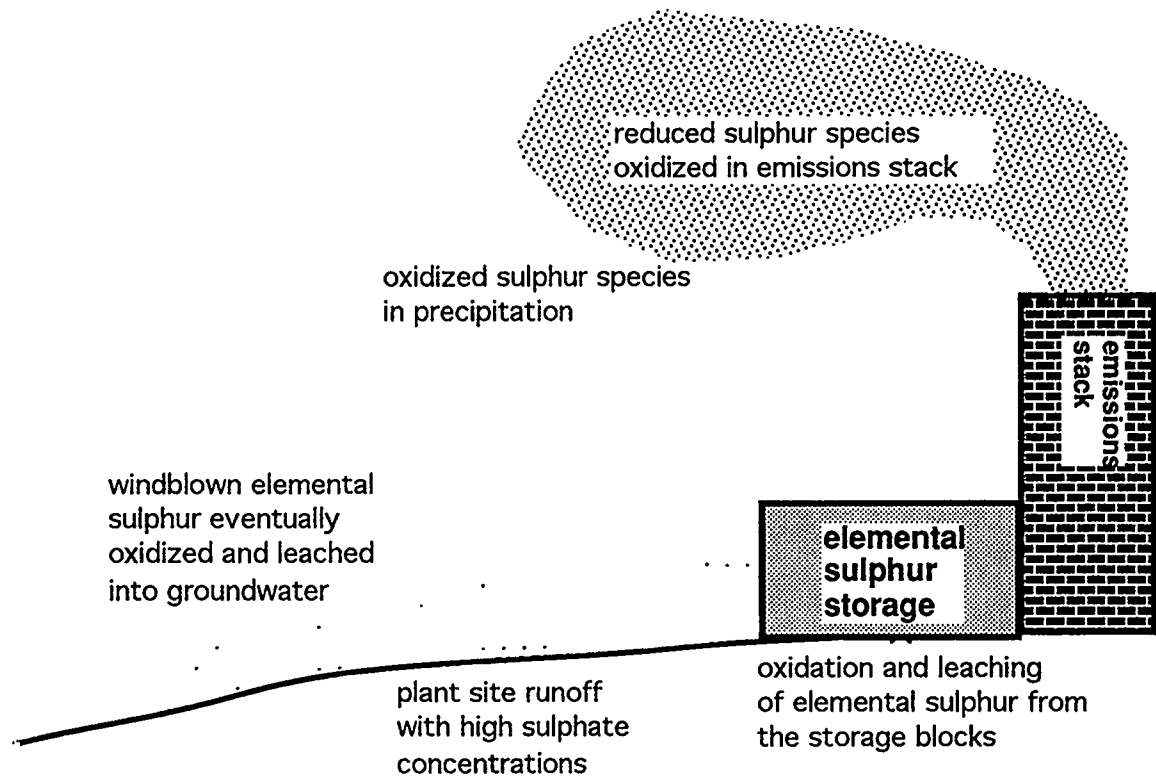


Figure 1.1: This cartoon illustrates the main processes which result in sulphate contamination of groundwater near sour gas plants.

Whereas, sulphur in oxygenated, shallow groundwater is found mainly as sulphate, in anoxic systems anaerobic bacterial reduction to sulphide can occur. Groundwater beneath or adjacent to sour gas processing facilities can have sulphate concentrations greater than 3000 mg/l. This is 2500 mg/l higher than the recommended Canadian water quality standard (CCREM, 1987). In addition to the deterioration of water quality, sulphuric acid can significantly alter water chemistry through water and rock interactions. Sulphuric acid comes from the oxidation of sulphur compounds, such as S⁰ (stock piled elemental sulphur) or SO₂ and H₂S (emissions from the stack).

Natural aqueous sulphate concentrations in shallow groundwaters in Alberta can exceed 1200 mg/l (Tokarsky, 1974). Because high concentrations of sulphate in groundwater may not indicate industrial contamination, high concentration alone is not adequate to establish whether sulphate is of natural or anthropogenic origin. In many situations, stable sulphur isotopes provide a means to distinguish between natural and anthropogenic sulphate.

Sulphur is found in various forms and valence states (from -2 to +6). It has four stable isotopes that are found on the earth surface with the following average percentages: ³²S-95.02%, ³³S-0.75%, ³⁴S-4.21%, and ³⁶S-0.02%. The relative amount of each isotope in a substance varies due to fractionation. Fractionation occurs because of mass differences between the isotopes.

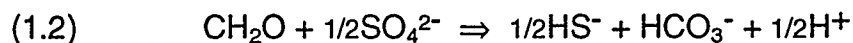
Stable isotope abundances are reported using δ (del or delta) values in parts per thousand (‰) or per mil (equation 1.1). The δ value expresses **R**, the ratio

of the number of heavy to the number of light atoms in a sample to that of an internationally accepted standard. For sulphur the abundance ratio (**R**) is expressed as $^{34}\text{S}/^{32}\text{S}$, for oxygen $^{18}\text{O}/^{16}\text{O}$ and for hydrogen it is D/H.

$$(1.1) \quad \delta_{\text{sample}} \text{‰} = \left[\frac{(\text{R})_{\text{sample}}}{(\text{R})_{\text{standard}}} - 1 \right] \bullet 1000.$$

The international standard used for sulphur is troilite from the Cañon Diablo meteorite (CDT). For oxygen and hydrogen, an approximation to Standard Mean Ocean Water is used as distributed by the IAEA (V-SMOW).

Variations in relative sulphur isotope abundances are primarily due to redox reactions in the bacterial sulphur cycle. Dissimilatory sulphate reduction, summarized in the reaction below, is ^{32}S and ^{16}O selective (e.g. Chambers and Trudinger, 1979).



Because biological sulphate reduction is isotopically selective, the remaining SO_4 pool becomes ^{34}S and ^{18}O enriched. Although the presence of bacteria can enhance sulphide oxidation rates, the process is negligibly isotope selective (e.g. Krouse, 1980).

In Alberta, anthropogenic sulphate originating from sour gas processing facilities that process H_2S from carbonate hosted reservoirs of Paleozoic age is relatively enriched in ^{34}S compared to the surrounding environment. This enrichment mainly reflects derivation of the H_2S from thermochemical reduction

of ancient marine anhydrite (e.g. Krouse et al, 1987). Therefore, H₂S processed at sour gas plants has $\delta^{34}\text{S}$ values ranging from +15 ‰ to +35 ‰. In contrast, natural terrestrial sulphate in Alberta glacial deposits is relatively depleted in ³⁴S. Typical $\delta^{34}\text{S}$ values range from +2 ‰ to -35 ‰ (Krouse, 1981, Hendry et al., 1986, van Donkelaar, 1991).

1.2 Past Work

The discussion of past work is limited to the use of $\delta^{34}\text{S}$ as a tracer of anthropogenic sulphur in Alberta and the use of $\delta^{34}\text{S}$ as a tracer of industrial sulphate in groundwater worldwide.

For nearly two decades, $\delta^{34}\text{S}$ values have been used in Alberta to trace anthropogenic sulphate in the atmosphere (Krouse and Case, 1983), precipitation (Norman, 1992), vegetation (Krouse, 1977), soils (Krouse and Case, 1981; 1983) and surface waters (van Donkelaar, 1991). The characteristic isotopic abundance of anthropogenic sulphur is retained by the oxidized sulphate since the transformation from S⁰ or SO₂ to sulphate has negligible S-isotope selectivity (e.g. McCready and Krouse, 1982). In addition to tracing anthropogenic sulphate, $\delta^{34}\text{S}$ and $\delta^{18}\text{O}$ data from glacial tills and pristine groundwaters (Hendry et al., 1986; 1989), natural springs (Staniasek, 1992, Krouse, 1976) and pristine rivers (Hitchon and Krouse, 1972) have provided clues to the origin of natural aqueous sulphate in Alberta. Case studies in Alberta are discussed in Krouse and Grinenko (1991).

Although $\delta^{34}\text{S}$ has not been used to trace anthropogenic sulphate in Alberta groundwaters, it has been used elsewhere. For example, researchers in southern Ontario (Robertson et al., 1989) and eastern Poland (Trembaczowski, 1991) took advantage of the difference between natural and anthropogenic sulphur $\delta^{34}\text{S}$ to identify sulphate sources in groundwater. In both of these studies, as well as the pristine groundwater studies mentioned earlier, biological sulphate reduction was recognized as an important process.

Sulphate reduction by microorganisms can have a significant impact on the $\delta^{34}\text{S}$ of remaining sulphate. The preferential reduction of $^{32}\text{S}^{16}\text{O}_4$ by sulphate reducers has been well documented, as has the resulting $\delta^{34}\text{S}$ enrichment in the remaining sulphate (e.g. Krouse, 1970; Rees, 1973). This leads to the question: is relative ^{34}S enrichment of aqueous sulphate indicative of sulphate from an industrial source or is it due to sulphate reduction by microorganisms?

1.3 Thesis Objectives

The objectives of this thesis are to:

1. Explore the reliability of sulphur isotope abundances as tracers of anthropogenic sulphate in groundwater using four independent approaches:
 - a) measure $\delta^{34}\text{S}$ and $\delta^{18}\text{O}_{\text{sulphate}}$ and look for enrichment due to preferential $^{32}\text{S}^{16}\text{O}_4$ reduction,

- b) measure the dissolved oxygen content of groundwater *in-situ* to assess the suitability of the system for sulphate reduction,
 - c) perform hydrogenase enzyme test for the activity of sulphate reducing bacteria (SRB) (Bryant et al., 1991),
 - d) incubate samples under warm (25°C) anoxic conditions and test for change in $\delta^{34}\text{S}_{\text{Sulphate}}$ after seven months.
2. Use $\delta^{34}\text{S}$ to trace anthropogenic sulphate in groundwater in a case study.
 3. Use geochemical and isotopic information to investigate how groundwater chemistry near a sour gas plant has changed due to high anthropogenic sulphate concentrations.

A site was chosen to reach the thesis objectives. Three main criteria for site selection were:

1. sulphate contamination of groundwater from sour gas (H_2S) processing
2. reliably installed piezometers in place
3. permission from the facility owners.

The study site is in south western Alberta. The owners agreed to participate in the study if the site remained anonymous. The sour gas plant facility has been in operation since the earlier 1960's and elemental sulphur, produced at the plant, is stored as blocks (\cong 10 m high, 350 m X 100 m). When the price for sulphur is low, more of the elemental sulphur is stored.

1.4 Methods

Table 1 lists the groundwater data acquired and the rationale for each acquisition. Sampling took place over a year, during the months of July 1992, November 1992, March 1993 and June 1993.

1.40 Field Methods

Except for piezometer nest 13 (Twin Butte, 1984), piezometers installed by KOMEX International (1991), were used to characterize groundwater flow and chemistry. A piezometer schematic is shown in Figure 1.2. The piezometer casings are topped with a heavy metal screw top which prevents contamination from the surface. In addition, the piezometer tube has a tightly fitted plastic cap. The sand grain size is between 10 and 20 thousandths of an inch, the screen slots have a 20 thousandths of an inch (0.5 mm) separation and width. The polyvinyl chloride (PVC) pipe itself was schedule 40 strength (proportional to pipe wall thickness).

The main objective of groundwater sampling was to characterize and collect representative samples of the aquifer water. This meant allowing for sufficient flushing (bailing), preventing cross-contamination between sample points and analyzing or preserving the samples as quickly as possible.

Aquifer samples were obtained using a ball seal PVC bailer. The bailer was thoroughly wiped with paper towels and rinsed with distilled water between sample selection. To insure a representative aquifer sample, piezometers were either bailed dry or at least five hole volumes of water were removed before

water sample collection, (Classen, 1982). Hole volumes were calculated by knowing the depth to the standing water, the inside diameter of the liner and the final depth of the piezometer. Sterile Nalgene® sample containers were rinsed several times with the aquifer water being sampled. These waters were then taken to the field lab for on-site analysis and sample preservation.

TABLE 1: Summary of Data Acquired and Rationale

<u>DATA</u>	<u>RATIONALE</u>
•hydraulic head	characterize groundwater flow direction and gradients
•dissolved oxygen & temperature	assessment for bacterial activity consideration and computer modeling of mineral saturation indices
$\delta^{18}\text{O}$ & δD	characterization of groundwaters, enrichment / depletion due to water / rock interactions, evaporation / condensation
• $\delta^{34}\text{S}$	trace anthropogenic sulphate, check relations with other ions and stable isotopes
• $\delta^{18}\text{O}_{\text{sulphate}}$	identify oxygen source in sulphate, check relations with other stable isotopes
•ions	characterize groundwaters and understand alteration due to water/rock interactions
•hydrogenase test	test for activity of sulphate reducing bacteria
•X-ray diffraction	estimate semi-quantitatively the of minerals present in subsurface samples
•X-ray fluorescence	estimate of total sulphur in soil samples

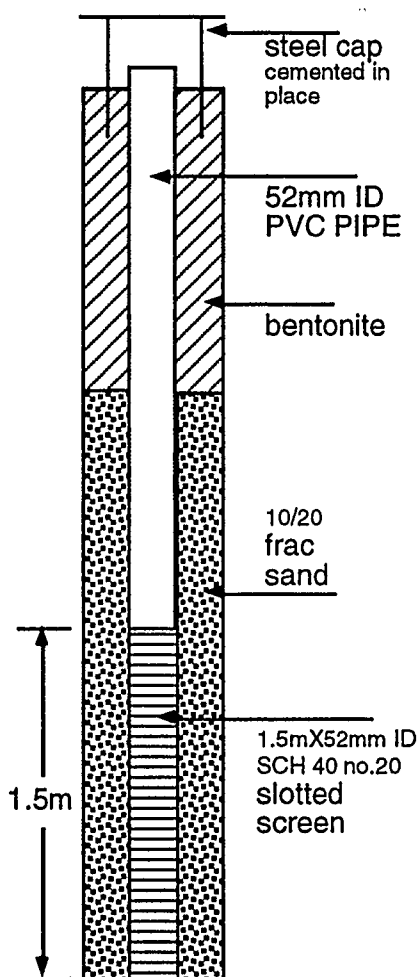


Figure 1.2: piezometer schematic

1.41 Field Sample Preservation

Water alkalinity and pH were measured on unfiltered samples immediately after collection using an Orion 960 auto-titrator. Two 60 ml Nalgene® (polypropylene) bottles of water were used for anion, δD , $\delta^{18}O$ and cation determination. Water was filtered ($0.45 \mu m$) using a Nalgene® 15 psi hand pump mounted on a 250 ml reservoir. To reduce cation complexing during storage and transport the samples for cation analysis were acidified to a pH of 2 with HCl. Anion water samples were also used for δD and $\delta^{18}O$ analyses.

The depth to groundwater was measured by lowering an electrical probe into the piezometer. Measurements to the top of the PVC liner were accurate to 0.5 cm. Dissolved oxygen and temperature were recorded using an air calibrated YSI 5739 Field Probe. The probe was corrected for temperature and elevation before each measure.

BaCl₂ crystals were added to filtered water samples in 100 ml glass bottles. This precipitated out SO₄ as BaSO₄, which is very stable. The samples were acidified (pH 2) to remove any BaCO₃ which may have also precipitated, (Staniasek, 1992). The presence of BaCO₃ can effect $\delta^{18}\text{O}$ analysis.

1.42 Laboratory

The July 1992 and November 1992 anion concentrations were measured at ambient temperature using a High Pressure Liquid Chromatograph (Department of Geology and Geophysics). The flow rate through the Water I.C.Pac Anion HC column was 2 ml/min. A borate gluconate buffer was used in the column. The March 1993 and June 1993 anion data were measured at the Institute of Sedimentary and Petroleum Geology (ISPG) in Calgary. The instrument and the procedures at the ISPG are identical to those at University of Calgary. Cation concentrations were analyzed using the acidified samples, on a Perkin Elmer 5000 atomic absorption spectrophotometer.

The analysis for $\delta^{18}\text{O}_{\text{sulphate}}$ followed the method of Shakur (1982). BaSO₄ is used for $\delta^{18}\text{O}_{\text{sulphate}}$ analyses because other minerals such as CaSO₄ may yield SO₂ when heated with graphite. The BaSO₄ precipitate was mixed with pure graphite (1:1 admixture) and heated to approximately 1000°C. CO₂ evolved from this reaction and was captured for $\delta^{18}\text{O}$ analysis. Any CO evolved was converted to CO₂ using a high voltage discharge cell. A detailed description of the procedure can be found in Shakur's Ph.D. Thesis p.51 (1982).

$\delta^{34}\text{S}$ analysis was performed using the methods of Yanagisawa and Sakai (1983) and Ueda and Krouse (1986). BaSO_4 precipitate was collected on 0.45 μm Millipore[®] filter paper, air dried and combined with vanadium pentoxide and silicon dioxide (1:20 $\text{BaSO}_4:\text{V}_2\text{O}_5/\text{SiO}_2$). This mixture was placed in a glass tube, topped with quartz fibers and copper and heated at 900°C for 30 minutes (hot copper reduces SO_3 to SO_2). Carbon dioxide was removed from evolving gas using a liquid N_2 pentane trap and water was frozen out with a dry ice bath. The SO_2 gas which evolved was immediately analyzed in a dual collector mass spectrometer built with V.G. Micromass 602 components (V.G. Micromass Ltd. Winsford, U.K.).

$\delta^{18}\text{O}$ of water was measured using a modified CO_2 equilibration technique of Epstein and Mayeda (1953). First, a 5 ml of sample water was equilibrated in evacuated tubes with reference CO_2 gas over night (>9 hours). Then the equilibrated CO_2 gas was analyzed on a triple collector 903 Micromass mass spectrometer (components from V.G. Micromass Ltd. Winsford, U.K.). This value was compared with the reference CO_2 relative abundance.

The procedure for δD analysis used the methods of Coleman et al (1982). A 5 μl water sample was added to 250 mg of Zn shot and heated to 450°C for 30 minutes. The H_2 gas which evolved was analyzed on a mass spectrometer constructed with Micromass 602 components (V.G. Micromass Ltd. Winsford, U.K.).

To measure the $\delta^{34}\text{S}$ soluble sulphate in soil, the soils were soaked and stirred in a 0.1 M LiCl solution for two days. The slurry was then filtered with 0.45 μm

filter paper and BaSO_4 precipitated from the filtered water using BaCl_2 (Dowuona et al., 1993). BaSO_4 precipitate was analyzed for $\delta^{34}\text{S}$ and $\delta^{18}\text{O}_{\text{sulphate}}$ as described above.

The soil material remaining on the filter paper after the soluble soil (aqueous sulphate) extraction, was used to obtain the $\delta^{34}\text{S}$ of the insoluble sulphate in soil. The samples were placed overnight in 600 ml beakers treated with 15 ml conc HNO_3 and 3 ml liquid Br_2 . The following day they were heated to dryness, 10 ml conc HCl was added and the samples were again evaporated to dryness. This procedure was repeated with another 10 ml of concentrated HCl . The samples were then diluted with distilled water, filtered and BaSO_4 precipitated from the filtered water using BaCl_2 (Krouse and Tabatabai, 1986). The BaSO_4 was used for $\delta^{34}\text{S}$ analysis as described above.

X-ray diffraction (XRD) and X-ray fluorescence (XRF) were performed on several soil and glacial till samples. The XRD analysis was performed using a Scintag XD5-2000. The instrument uses a copper tube and for the analysis it was set at 44 kV and 44 mamps. Clays present in the samples were not resolved, therefore the main XRD peaks identified were quartz, calcite, feldspars, clay and in some cases gypsum. Correction factors were selected from work by Bayliss (1986) and the analysis was aided by JADE software (Material Data Inc., 1993). Because of overlap in peaks, XRD is considered semi-quantitative at best. XRF analysis was done using a Philips PW1410. The instrument uses a rhodium tube and was set at 40 kV and 60 mAmps for the analysis.

The activity of sulphate reducing bacteria was assessed by measuring the hydrogenase enzyme concentrations (Bryant et al., 1989;1991, Costerton et al., 1989). The enzyme hydrogenase is associated with sulphate reducing bacteria. The hydrogenase test was performed by Dr. Ed Laishley (Biology Department, University of Calgary). The results are graded from 0 to 3, where 0 means that any bacteria present are inactive and 3 indicates strong activity. This test was done on the March 1993 sample set.

TABLE 2: DATA SUMMARY

	del 34S (SO4) CDT	del 18C (SO4) SMOW	del D (H2O) SMOW	del 18O (H2O) SMOW	Ca	Mg	Na	K	Mn2+	Fe2+	SO4	Cl	NO3	HCO3	pH	temp. oC	D.O.* mg/l	groundwater elevation (m)
	all ion concentrations: mg/l																	
s2A	13.4	5.9	-142.1	-16.9	464	105	28.0	2.2	0.20	0.09	922	0.0	0.0	636	6.9			1488.53
f2A	12.4	-1.8	-138.9	-17.3	467	102	8.5	2.1	0.00	0.09	1027	7.1	72.7	604	6.3	7.0		1488.25
f2B	-7.3	-	-161.8	-18.6	114	36	81.0	2.9	0.00	0.10	334	14.0	0.0	322	6.3			1485.32
s4B	14.8	-5.7	-125.4	-16.3	448	140	34.0	2.0	15.00	1.84	1094	0.0	0.0	574	7.8			1470.73
f4B	17.5	7.7	-131.7	-16.5	403	151	38.0	2.3	0.70	0.21	1185	14.0	0.0	403	6.5	7.0		1470.01
j4B	17.1	-20.7	-134.1	-17.5	437	144	28.2	1.9	12.10	3.10	1214	50.8	6.5	428	8.0	7.5	0.8	1471.26
s4C	3.9	-	-141.9	-18.6	101	41	21.7	2.1	0.20	0.09	50	39.6	0.0	369	7.9			1469.82
f4C	2.4	4.8	-143.4	-18.5	103	42	23.3	2.1	0.01	0.63	78	57.0	11.3	278	6.5	8.0		1469.95
w4C	-1.1	1.5	-142.8	-18.0	107	42	20.7	2.4	0.15	0.12	48	59.5	0.0	278	7.1	8.0	1.1	1469.53
j4C	6.0	-15.5	-136.7	-19.6	104	42	21.5	2.6	0.10	0.30	44	62.8	0.0	505	7.9	9.0	1.1	1470.55
s5A	15.2	-9.5	-125.3	-14.5	634	604	28.0	12.0	0.36	0.11	2767	0.0	0.0	435	7.6			1474.09
f5A	14.0	-11.8	-125.6	-15.3	542	698	29.0	9.7	0.01	0.19	3109	12.4	63.5	514	7.0	4.5		1472.35
j5A	16.7	-18.9	-126.8	-14.8	654	670	25.9	13.5	0.23	0.28	3397	0.0	0.0	780	7.7	12.1	0.6	1474.30
s5B	15.5	-7.1	-144.0	-18.2	459	259	10.3	2.3	6.47	1.42	1397	40.7	0.0	630	7.7			1469.62
f5B	15.1	-12.6	-140.8	-17.3	451	264	11.6	2.4	0.51	0.44	1816	38.5	0.0	512	6.3	7.5		1468.63
w5B	16.9	-1.1	-141.9	-17.5	432	239	8.8	2.4	5.75	0.71	1426	39.3	0.0	477	6.1	10.0	1.0	1468.50
j5B	17.4	-23.2	-140.6	-17.3	434	250	9.9	2.2	5.74	0.21	1589	42.2	0.0	857	7.2	11.0	0.7	1469.24
s5C	12.7	-7.1	-144.2	-18.4	221	78	61.2	2.7	0.44	0.39	445	10.3	0.0	386	7.8			1469.78
f5C	14.0	-9.4	-143.5	-18.4	183	64	35.9	2.4	0.03	0.59	349	37.4	15.6	513	7.0	8.0		1468.81
w5C	17.9	-11.0	-144.7	-17.9	437	133	17.7	3.0	0.39	0.35	956	29.2	0.0	512	6.7	10.0	1.1	1468.56
j5C	14.3	-20.1	-142.5	-18.3	194	66	18.7	2.5	0.18	0.07	293	77.7	0.0	636	7.4	10.9	2.8	1469.44
s6C	-5.6	-	-147.5	-19.4	85	36	29.6	1.9	0.11	0.23	34	0.0	0.0	368	8.0			1468.45
f6C	-6.0	3.4	-145.2	-19.1	76	33	29.5	2.0	0.01	0.07	38	26.8	39.9	253	6.6	7.5		1468.08
w6C	-6.2	11.0	-148.1	-18.8	85	35	25.4	2.1	0.04	0.11	31	27.6	0.0	277	6.7	7.0	1.2	1467.56
j6C	6.5	10.4	-145.5	-19.1	87	36	27.2	2.2	0.03	0.07	20	35.9	0.0	494	7.6	7.5	2.4	1468.33
s7B	11.4	2.5	-141.4	-18.2	142	78	8.0	2.9	0.03	0.03	165	74.3	33.5	438	7.8			1470.26
f7B	13.1	-	-139.0	-18.1	124	68	15.8	2.2	0.00	0.10	104	50.9	0.6	334	7.1	7.5		1468.95
w7B	14.8	-1.7	-139.1	-17.7	174	82	12.9	2.8	0.04	0.02	159	106.5	15.4	357	7.0		2.3	1467.79
j7B	12.0	-16.6	-142.4	-17.7	133	76	25.7	2.5	0.03	0.08	211	56.8	0.0	740	7.9	10.2	3.9	1470.58
s7C	15.2	-7.4	-142.8	-17.6	460	207	26.6	2.3	4.27	0.08	1278	24.2	0.0	630	7.6			1462.97
f7C	15.1	-9.3	-142.5	-17.4	400	178	26.7	2.6	0.27	0.35	1193	34.0	24.7	472	6.5	6.0		1462.49
w7C	17.7	-	-140.3	-17.0	445	188	18.8	2.8	4.02	0.15	1237	36.2	0.0	469	6.4	7.5	2.0	1461.87
j7C	17.3	-24.4	-138.1	-17.4	378	168	18.3	2.2	3.09	0.27	1179	44.8	0.0	781	7.6	7.9	1.0	1462.94
s13N	15.0	-	-146.5	-16.1	328	123	25.0	3.1	1.21	0.44	1254	31.9	0.0	574	6.9			1482.15
f13N	15.8	4.4	-144.2	-16.0	279	104	21.4	2.8	0.10	0.07	835	60.7	44.2	305	6.2	6.0		1479.98
w13N	18.3	4.5	-142.7	-15.0	361	132	22.2	3.3	1.24	0.57	1405	62.6	0.0	318	6.7	7.5	2.0	1479.67
s#1	-11.4	-10.5	-141.2	-18.4	114	32	7.9	2.3	0.02	0.05	64	0.0	0.0	208	8.2			1491.20
f#1	-11.8	4.9	-140.9	-18.3	98	28	14.9	2.3	0.00	0.08	88	2.5	0.0	265	7.4	5.0		1491.20
w#1	-13.9	3.5	-143.3	-18.0	124	34	4.8	2.4	0.03	0.03	75	3.2	0.0	392	7.0			1491.20
s-rain	15.6	6.0	-105.5	-14.9	10	1	0.1	0.1	0.02	0.04	15	0.0	0.0	-	-			0.00
j#9a	16.6	-13.5	-132.8	-17.5	219	60	17.4	1.9	0.03	0.10	417	110.7	0.0	475	7.7			1455.80
j-res	-	0.9	-138.5	-18.4	31	11	1.7	0.7	0.03	0.06	24	0.0	0.0	190	7.4			1450.00
s13S**	14.2	2.1	-158.0	-15.8	394	86	26.7	4.3	1.87	0.15	896	16.5	0.0	386	7.5			1481.34
f13S	14.2	1.1	-151.7	-15.1	348	81	25.0	3.8	0.12	0.58	1150	57.5	04.8	333	6.6	5.8		1480.82
w13S	16.4	1.3	-158.4	-14.3	401	87	26.0	5.9	1.80	0.11	855	55.0	0.0	428	6.5	8.0	1.8	1480.65
j6B	17.3	-19.0	-148.6	-16.0	>>>> insufficient sample for A.A. <<<<							1638	132.7	7.3	353	7.4		1468.55

**problematic ion concentrations discussed in Chapter 3

*dissolved oxygen

CHAPTER 2: SETTING

2.1 Climate

The climate in the area is characterized by short cool summers and cold winters. Cloud bursts, high winds and thunder showers are common in the summer. July, the warmest month, has a mean temperature of about 17°C. January has a mean temperature of -8°C. Throughout the year, warm winds (Chinooks) occasionally blow in from the west coast and increase the temperature by 10°C or more.

Based on data collected from 1987 to 1991 by Parks Canada and the Town of Pincher Creek, mean annual precipitation near the plant site is 814 mm while evapotranspiration is approximately 400 mm/yr, (Tokarsky, 1974). As shown in Figure 2.1, about 14% of the yearly precipitation falls in June. Groundwater temperature extremes of 4.5°C and 12°C were measured in the shallowest piezometer 5A, (samples f5A and j5A).

2.2 Topography

Approximately four kilometres west of the study site is the sharp relief of the Rocky Mountain Front Ranges. Nearby mountains reach elevations of up to 2470 m and creeks and rivers drain steep NE trending canyons. The gas plant site, at an elevation of 1490 m, is on top of a knoll that is bordered by two of these N-NE flowing creeks.

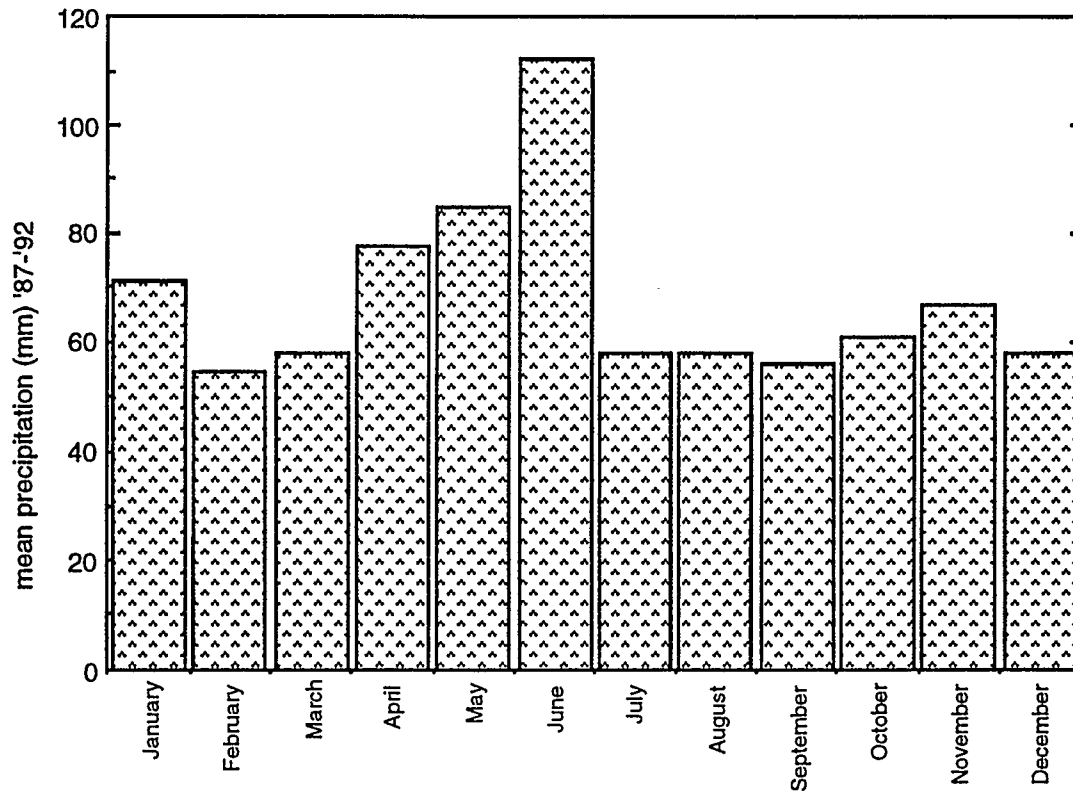


Figure 2.1: This bar chart shows mean precipitation in each month based on data collected from 1987 to 1991.

The study area, shown in Figure 2.2, is limited to the southern side of the gas plant knoll and surrounds the sulphur storage and processing area. There are 13 piezometer installations which are screened at depths ranging from 3 m to 21 m. The ground slopes gently towards the south, where it drops steeply into the creek. The creek under-fits the northeast trending valley it flows through. Steep banks cut through the glacial over-burden and expose the contact between glacial till and bedrock. About 20 years ago the creek was dammed just south of piezometer 4 to form a water reservoir for plant site operations.

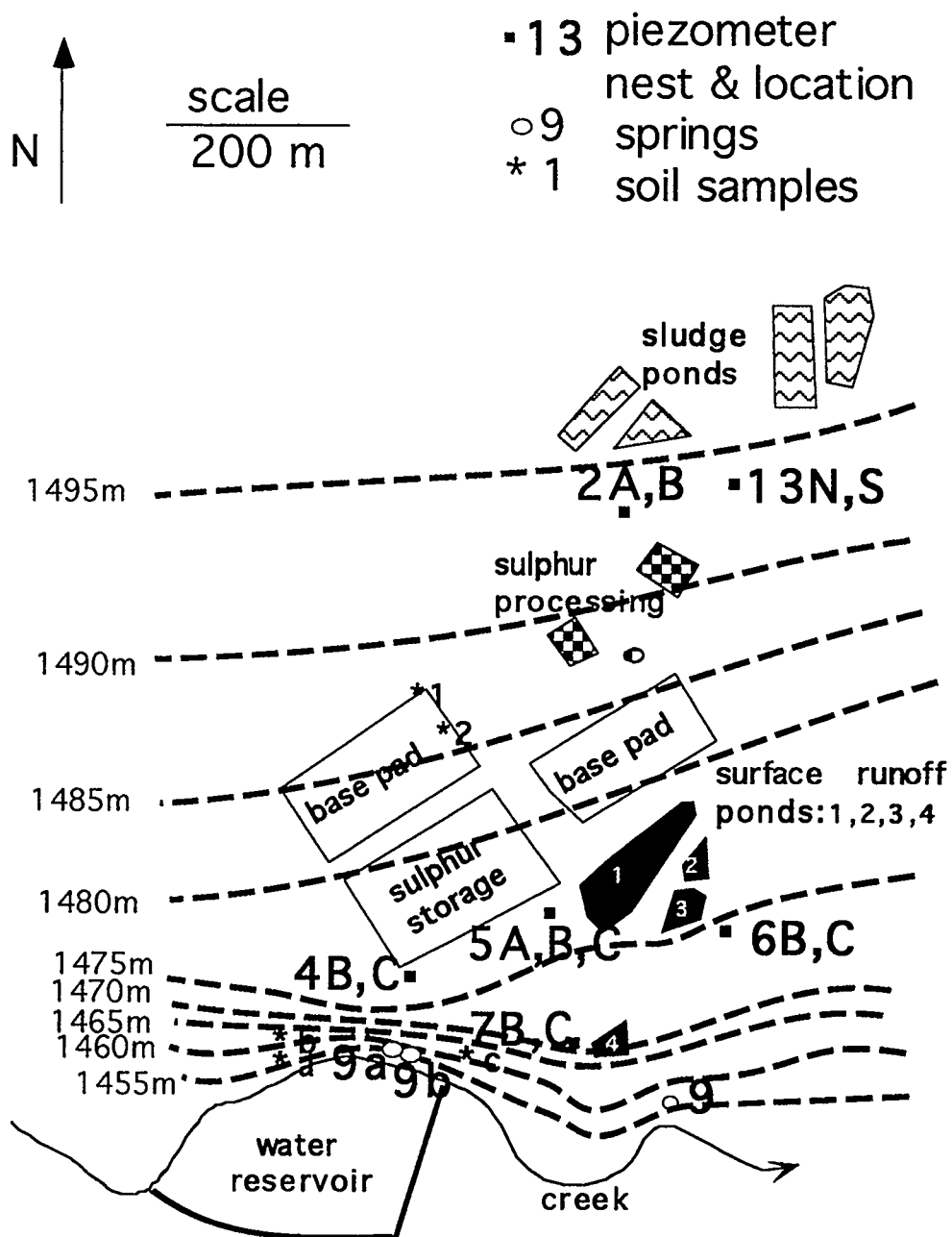


Figure 2.2: The study area covers the south side of the gas plant site and surrounds the sulphur storage and processing area.

2.3 Geology

The Cordilleran ice sheet, which covered the region during the last ice age, retreated back towards the Rocky Mountain front ranges about 10,000 years ago (Stalker, 1977). The glacial material left behind originated from the west and therefore contains fragments and rock flour of ancient rocks found in the Rocky Mountains, such as limestone and dolomite. Typically the glacial deposits are comprised of a heterogeneous mixture of silty and sandy clays, quartz sands, gravel and/or rock flour. Gravelly glacial outwash channels also are present. Work by the Alberta Research Council characterized the upper soil zone (1 metre depth or less) in the region as clayey to fine loamy, meaning that the clay content of the soil was 18 % or more (Holowaychuk et al., 1987).

The geologic model for the study area is based primarily on the drill cutting descriptions from piezometer installation (KOMEX, 1991). Figure 2.2 shows the locations of the piezometers, and, as indicated by the drill cuttings logs (Figure 2.3), the study area is underlain by 12 to 22m of alternating glacial silts, gravel and clays. The upper two metres tend to be gravel fill and sandy silt which has been disturbed by plant site construction. Below the gravel is five to eight metres of rust stained or weathered clayey silt which lies above about five or more metres of interbedded glaciolacustrine silts and clays.

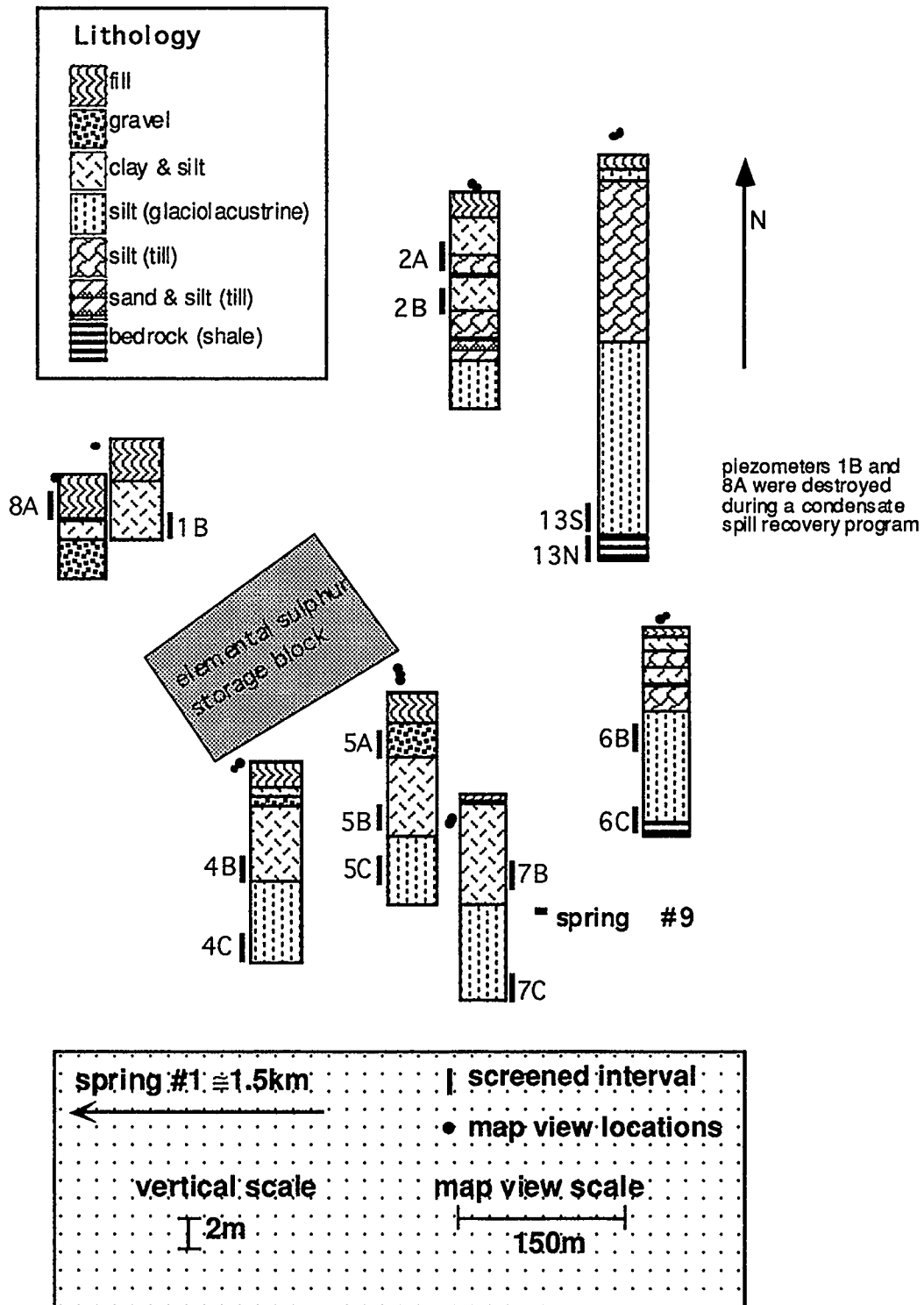


Figure 2.3: Drill cutting logs illustrate the heterogeneity of the glacial deposits. Also shown are the screened intervals.

A consultant's report for the base pad northwest of piezometer nest 4 describes a buried gravel channel overlying bedrock which disappears to the southeast (HBT AGRA, 1993). Several two metre deep test pits from the same report show a predominance of alternating clays and fine silts. The test pits were refilled after sampling. This report and Figure 2.3 demonstrate that it is not uncommon for glacial stratigraphic units to pinch out between sampling points.

In addition to the drill cutting logs, three samples of glacial deposits were dug out of the water reservoir banks south of the gas plant (Figure 2.2: *a,*b,*c). Averaged X-ray diffraction (XRD) results indicate a predominance of quartz (80 %), with about 5 % calcite, 5 % feldspar and 10% various clays (illite, kaolinite or smectite). It should be noted that quartz abundances are often exaggerated by XRD and that mineral weight percent estimates are not very accurate.

The bedrock, Upper Cretaceous Wapiabi Formation, slopes gently towards the southeast. The bedrock consists of alternating zones of fissile, dark grey to black, silty and sandy marine shales. In places it contains sideritic concretions, minor siltstone, sandstone and limestone. Piezometers 13N and 6C are the only piezometers in the study area which encountered bedrock, according to these cutting logs, the bedrock is a dark grey silty shale. Also, the shaley bedrock was drilled by HBT AGRA (1993) below the base pad north west of piezometer 4. A three point problem using depth to bedrock from 13N, 6C and the base pad bedrock indicate that the bedrock dips at approximately 2° towards 150° (SE).

2.4 Hydrogeology

The glacial material at the site blankets the less permeable bedrock below, so that recharging water moves downward, follows the southeast dipping bedrock and discharges along the creek banks. Figure 2.4 is a cartoon illustrating the general direction of groundwater movement.

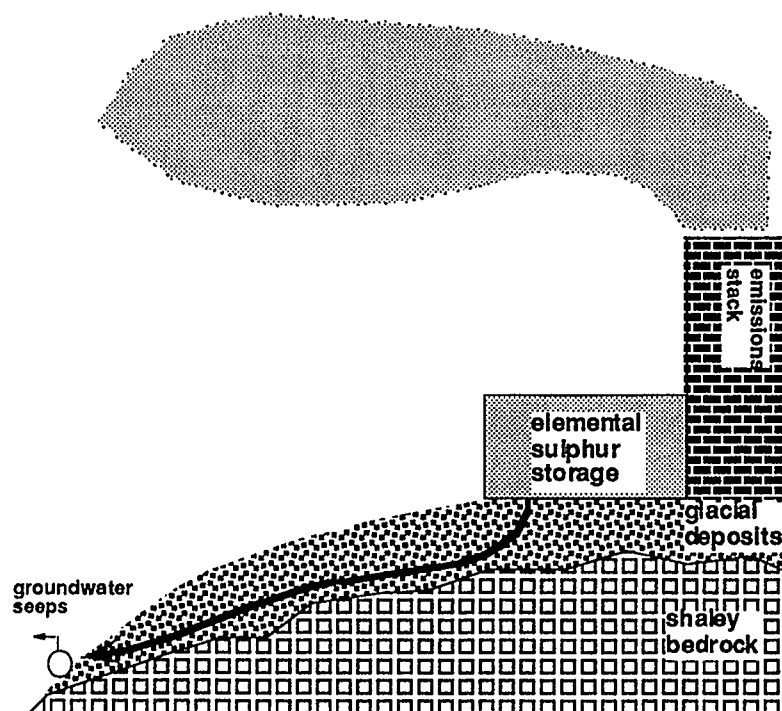


Figure 2.4: This cartoon illustrates simplified groundwater movement downward through the glacial deposits and along the bedrock.

The background sample (spring #1) is located 1.5 km west (upwind) of the sulphur storage pads. The exit point of the spring is within highly weathered

bedrock exposed in a road cut. The glacial till / bedrock contact is approximately 2 m above the discharge point. The ion concentrations from this sample point (Table 2), are consistent with pristine shallow groundwaters in the area (Tokarsky, 1974).

Hydrogeologic information includes hydraulic conductivities for 7 of the 13 piezometers and hydraulic head measurements for most of the piezometers over four sampling sessions, Table 3. Figure 2.4 illustrates the seasonal variation in head measurements, confirming this as a transient system. Groundwater elevations rise in the early summer months, coincident with the highest precipitation.

Three hydrogeologic zones at the site are defined as: (A) an upper zone comprised of approximately three metres of disturbed sand and gravel, (B) a middle zone of five to eight metres of silty sands and clays, and (C) glaciolacustrine silty clay down to bedrock. These zones are used for name references, for example 5A is shallower than 5B. Also, the sampling session is identified using the following prefixes, July 23, "s", November 11, "f", March 7, "w", June 21, "j". Piezometers 13S and 13N were installed in 1985 and are both screened over interval C. The designations "N" and "S" refer to north and south, respectively. A strong vertical gradient exists between zones A and B (Table 3); however, near the glacial / bedrock contact the vertical gradient is close to zero and groundwater movement is predominantly horizontal towards the water reservoir and the creek.

TABLE 3: Hydrogeology Data Summary

groundwater elevations (m)							
	July 23 1992 (m)	Nov.11 1992 (m)	Mar.7 1993 (m)	Jun. 21 1993 (m)	screen from (m)	to (m)	K** (m/s)
2A	1488.53	1488.25	1487.83	N/A*	1489.96	1488.46	3.80E-07
2B	dry	1485.32	dry	N/A	1487.48	1485.98	
4B	1470.73	1470.01	1469.94	1471.26	1472.00	1470.50	
4C	1469.82	1469.95	1469.53	1470.55	1467.56	1465.96	3.50E-07
5A	1474.09	1472.35	1471.94	1474.30	1474.13	1472.63	3.00E-08
5B	1469.62	1468.63	1468.50	1469.24	1470.05	1468.55	
5C	1469.78	1468.81	1468.56	1469.44	1467.02	1465.52	7.90E-08
6B	dry	dry	dry	1468.55	1470.48	1468.98	
6C	1468.45	1468.08	1467.56	1468.33	1463.30	1461.80	3.60E-06
7B	1470.26	1468.95	1467.79	1470.58	1469.19	1467.69	3.00E-08
7C	1462.97	1462.49	1461.87	1462.94	1462.42	1460.92	1.00E-06
13N	1481.29	1479.98	1479.67	N/A	1472.90	1471.40	
13S	1482.20	1480.82	1480.65	N/A	1472.95	1471.45	
#1	1491.20						

*Not Accessible
**hydraulic conductivity

vertical gradients positive downward				
	July 23 1992	Nov.11 1992	Mar.7 1993	June 21 1993
2A,B		0.99		
4B,C	0.20	0.01	0.09	0.16
5A,B	1.10	0.91	0.84	1.24
5B,C	-0.05	-0.06	-0.02	-0.07
6B,C				0.03
7B,C	1.08	0.95	0.87	1.13
13N,S	0.45	0.42	0.49	

The reduction in vertical gradient coincides with the depth of the silty more hydraulically conductive unit: zone C. The groundwater flow can therefore be further simplified to a two layer system comprised of an upper low conductivity

horizon (zones A and B) overlying a more conductivity, relatively continuous silty unit (zone C). Figure 2.6 shows the March 7, 1993 hydraulic head map for zone C. Zone C (the zone resting on bedrock) is used for hydraulic head mapping because the vertical gradient is close to zero.

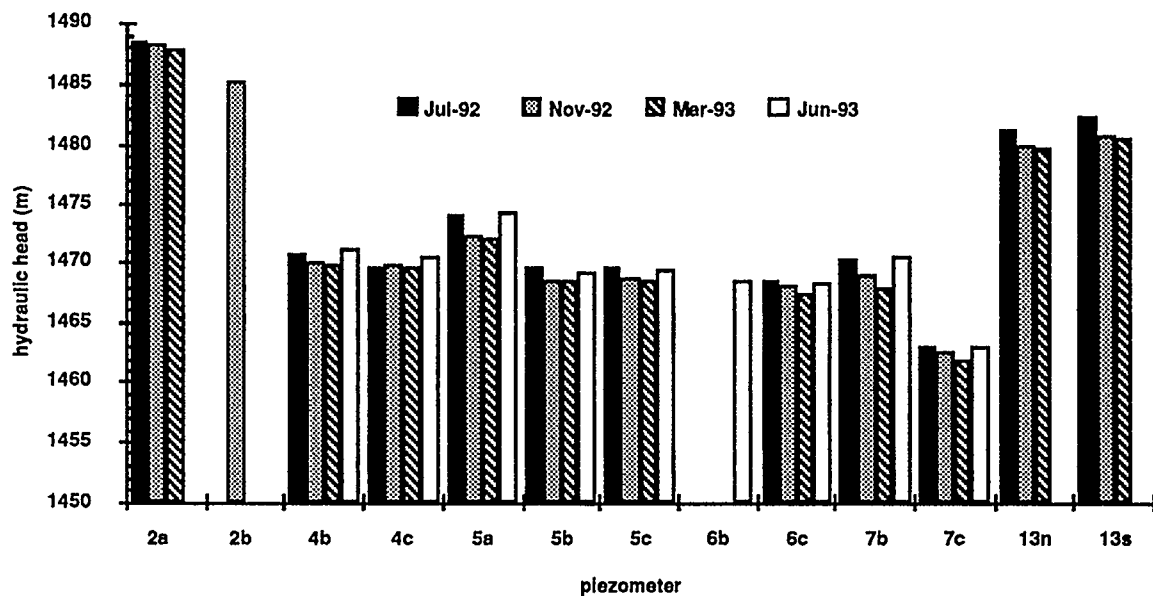


Figure 2.5: Bar graph of piezometer head variation with the season, groundwater elevations rise in the early summer months when precipitation is greatest.

Groundwater discharges, in the form of seeps, are present south of piezometer nests 4 and 7 where the water reservoir cut bank exposes the contact between the till and the bedrock. One of these seeps, #9a, was included in the June 1993 sampling program.

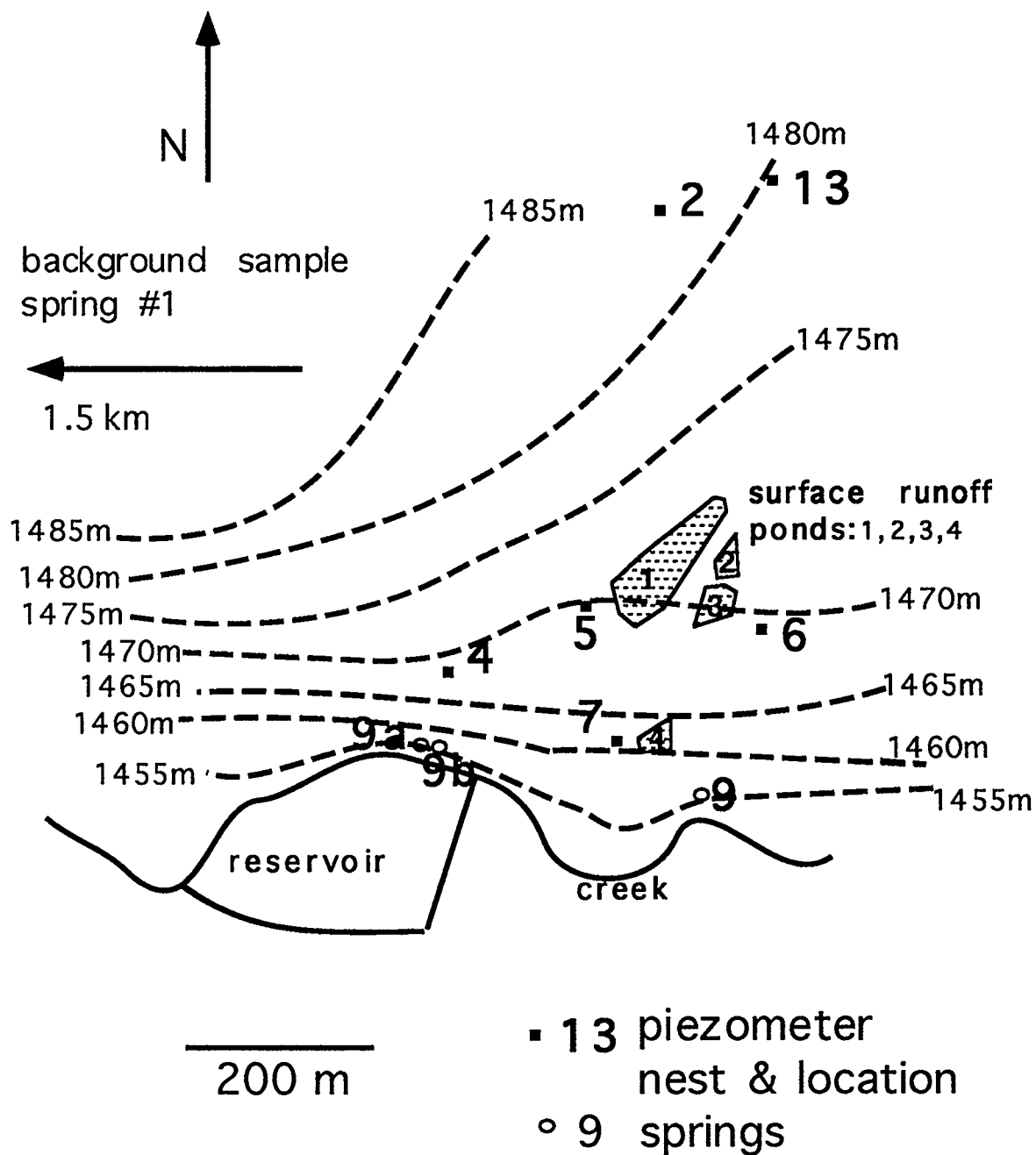


Figure 2.6: Hydraulic head for zone C resembles surface topography. Note contour deflections near surface runoff ponds (1,2,3,) indicative of water table mounding.

Groundwater levels part way up the screened intervals were measured in piezometers 2A, 4B, 5B, 6B and 7B (Table 3). These water levels also varied considerably with the season, for example the hydraulic head of w7B (1467.79 m) j7B (1470.58 m) differ by 2.8 m. This large variation in head and the occurrence of water levels part way up the screened intervals indicates that the screens cross the unsaturated / saturated zone contact. The screened interval in piezometer 6B was above the water table in all but one sampling session (j6B). The vertical gradient between j6B and j6C is low.

Two groundwater travel times were needed. First, the approximate time from recharge (water table) to the sampling point (piezometer screens) was required for incubation experiments (Chapter 4). Second, the residence time from recharge to discharge (e.g. spring #9) was needed to test the continuity of low hydraulic conductivities (10^{-7} m/s). The calculated residence time was compared with a known residence time from the sulphur pad to spring #9.

The residence time calculation was split into vertical (e.g. 7 m from 5A to 5C) and horizontal components (approximately 242 m from sulphur pads to spring #9). Residence time was calculated using the equation and data outlined below:

$$(2.1) \quad V = K \cdot \frac{i}{n_e} = \text{GROUNDWATER VELOCITY m/s (AVERAGE LINEAR)}$$

where: K = hydraulic conductivity m/s

$$10^{-5} < \text{zone C horizontal } K < 10^{-7} \text{ m/s (KOMEX, 1991)}$$

$$10^{-6} < \text{vertical } K < 10^{-9} \text{ m/s (Domenico and Schwartz, 1990)}$$

$i = \text{gradient}$

$0.048 < \text{horizontal } i < 0.050$ (5C to 7C)

$0.02 < \text{vertical } i < 1.2$ (Table 3)

$n_e = \text{effective porosity} = 0.03 \text{ to } 0.05$ (KOMEX, 1991)

$$(2.2) \quad R = \frac{d}{V} = \text{RESIDENCE TIME}$$

where: $d = \text{distance} = 7\text{m vertically \& } 242\text{m horizontally}$

Piezometer nests 4 and 5, which are adjacent to the sulphur pads, were used to estimate a range of vertical gradients (Table 3), while piezometers 5C and 7C were used for horizontal gradients. Zone C, in which most of the horizontal transport occurs, has hydraulic conductivities from bail tests ranging from $>10^{-6}$ to $\cong 10^{-7}$ m/s (KOMEX, 1991). Vertical hydraulic conductivities are assumed to be ten times the horizontal values (Domenico and Schwartz, 1990). Minimum and maximum residence times were calculated using extremes in hydraulic conductivity, gradient and effective porosity.

The calculated residence time was compared to a known travel time. Spring #9, which is 242 m south of the sulphur pads, was first sampled 22 years after the gas plant began operations. Extremely high sulphate concentrations (>1400 mg/l) indicates that the residence time from the sulphur pads to spring #9 must be less than 22 years.

The calculated vertical travel time (water table to sampling screens) ranged from 2 days to 554 years. The calculated residence time (vertical + horizontal) ranged from 0.5 to 635 years. The calculated maximum residence time is almost 30 times greater than the known maximum of 22 years suggesting that at least one of the variables used for the estimate is wrong.

Hydraulic conductivity significantly affects the resident time calculation and is typically accurate to within an order of magnitude. Therefore, it is likely that hydraulic conductivity between the sulphur pads and spring #9 is on average ten times greater than the lowest value (10^{-7} m/s) from bail tests. Intermittent zones of weathering and fracturing are often present in Alberta's glacial deposits (Hendry et al., 1986). Indeed, partings and joints up to 0.5 mm wide were observed in undisturbed clay till samples taken at \cong 5 m depth from the northeast corner of the plant site (Twin Butte, 1984). These fractured zones would have rapid groundwater flow. Also, the heterogeneity of the glacial deposits at this site could cause large variations in not only hydraulic conductivities but also effective porosities and gradients. Finally, the source of sulphate contamination in spring #9 could be closer than the sulphur block so that the travel time from the sulphur block to spring #9 is actually longer than 22 years. For example, the surface catchment ponds are \cong 100 m closer to spring #9 than the sulphur block.

In summary, both the topography and bedrock at the site dip gently towards the southeast. Glacial deposits blanket the bedrock with a heterogeneous mixture of silt, sand and clay, that includes discontinuous lenses and layers. Within the

glacial till a strong vertical gradient dominates the groundwater movement; this vertical gradient is close to zero as the recharging water approaches the glacial/bedrock contact. Horizontal flow is along bedrock towards the southeast. Therefore, shallow groundwater recharges on the gas plant knoll and discharges on the creek banks in the southeast. An estimate of the maximum groundwater residence time from the sulphur pads to spring #9 (on the creek banks) was an order of magnitude greater than the known residence time. It is possible that the discrepancy between the estimate and the actual residence time is due to high conductivity units within the glacial till.

CHAPTER 3: GEOCHEMICAL AND ISOTOPIC DATA, OBSERVATIONS AND TRENDS

The following chapter provides an overview of the data gathered for this study. Groundwater samples were collected and analyzed as described in Chapter 1 and the data are summarized in Table 2. The chemical composition of the groundwater surrounding the sulphur block is very different from the pristine samples taken from spring #1. Spring #1, which is 1.5 km upwind from the gas plant, has a Ca-Mg-HCO₃ composition with low ion concentrations typical of pristine groundwater in the area. Most of the groundwater samples collected near the sulphur pads are Ca-Mg-SO₄ with ion concentrations 10 to 100 times greater than pristine groundwater.

3.1 Ionic Strength

The ionic strength of a solution is a measure of the strength of the electrostatic field caused by ions in solution. It is calculated using equation 3.1:

$$(3.1) \quad I = \frac{1}{2} \cdot \sum m_i z_i^2$$

where: I = ionic strength (mmol/kg)
 m = molality of an ion in solution (mmol/kg)
 z = charge on the ion

The ionic strength of the groundwater samples ranges from 0.011 mol/kg (w6C) to 0.175 mol/kg (j5A). In particular, ionic strength is greatest near the sulphur

storage block. As shown in Figure 3.1, ionic strength varies considerably between sample points and with the season.

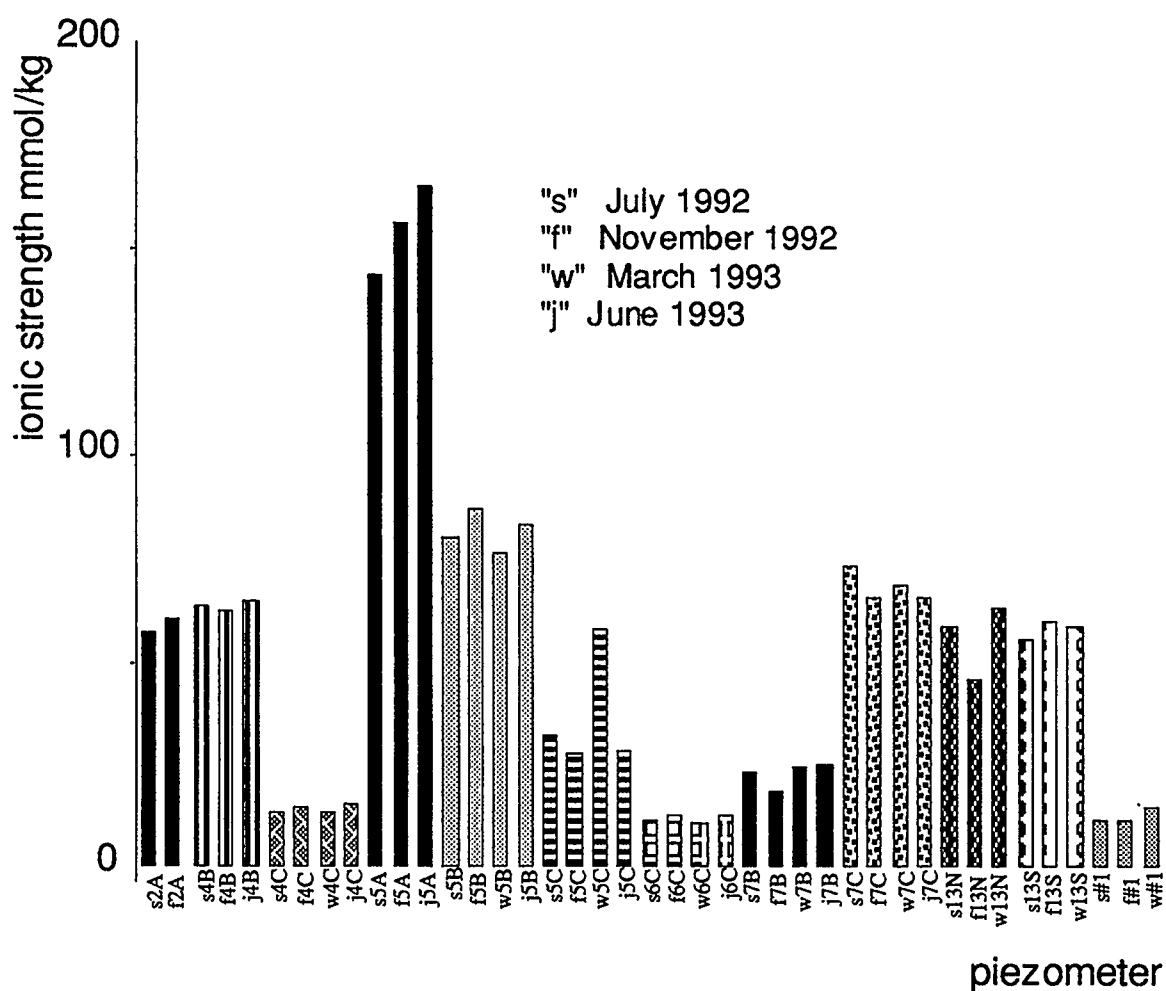


Figure 3.1: Ionic strengths vary throughout the year.

Figure 3.2, shows that ionic strength correlates well with sulphate concentration.

The lower ionic strengths are found in the more pristine samples.

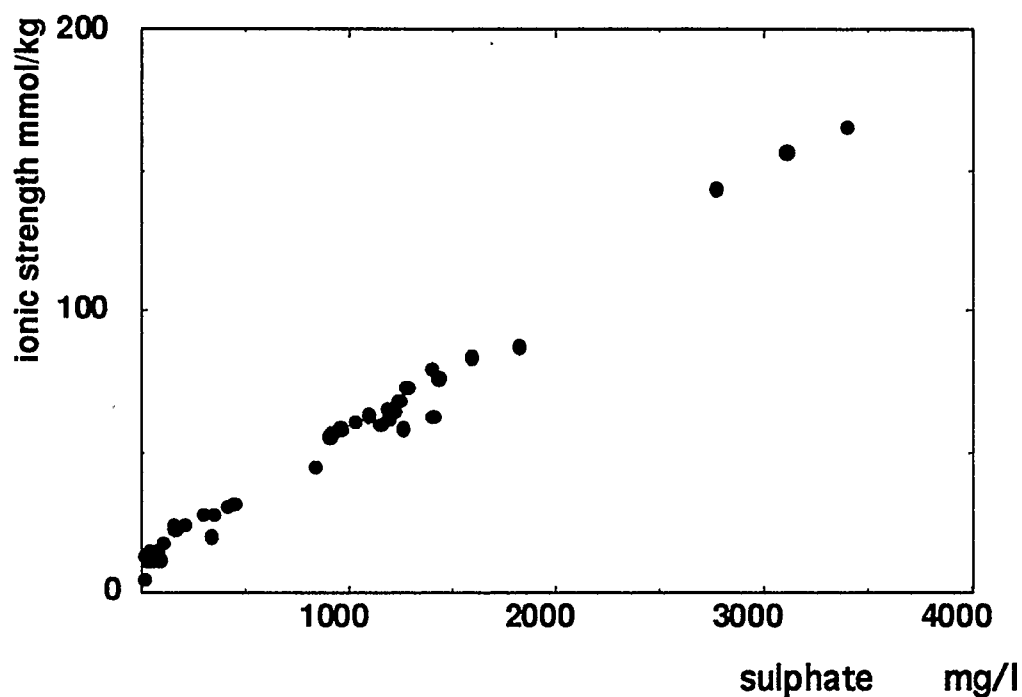


Figure 3.2: Groundwater ionic strength as a function of sulphate concentrations.

3.2 Sulphate Concentrations

As illustrated in Figure 3.3 increases in sulphate concentrations are accompanied by increases in calcium and/or magnesium concentrations. The calcium and sulphate concentrations correlate very well, suggesting that they are inter-dependent on the other. Similar (albeit less distinct) relations are found between sulphate and other cations, such as sodium.

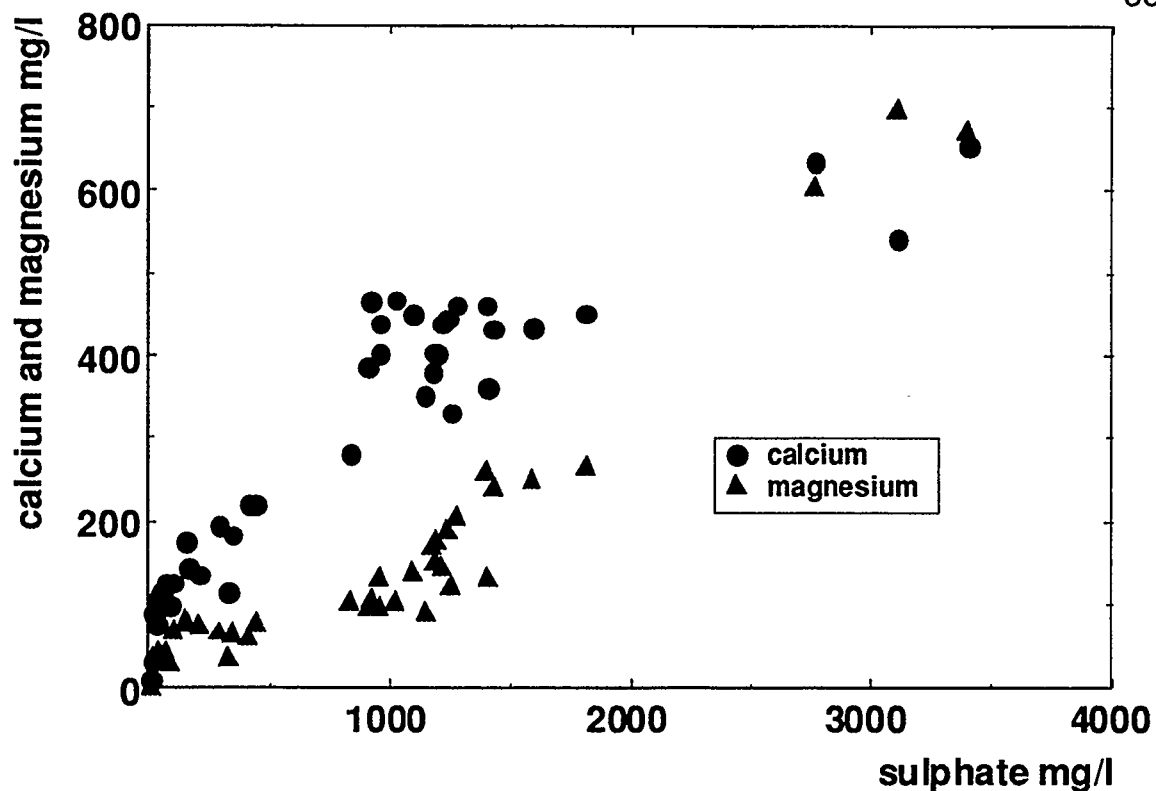


Figure 3.3: Increases in sulphate concentrations are accompanied by increases in calcium and magnesium concentrations.

Sulphate concentrations in the groundwater samples from the piezometers are usually greater than those observed in spring #1 (pristine sample). Piezometers 4C and 6C have the only groundwater sulphate concentrations close to pristine groundwater. Elevated sulphate concentrations are found near the obvious sources (e.g. the sulphur blocks), and near the not so obvious, such as the abandoned sludge ponds near piezometer nest 13. Piezometers 5A and 4B, which are shallow samples points close to the sulphur pads, have groundwater samples with extremely high sulphate concentrations, 3397 mg/l and 1214 mg/l, respectively.

Piezometer 7C is several hundred meters southeast of the sulphur pads and has sulphate concentrations as high as 1278 mg/l (s7C). Sulphate concentrations an order of magnitude less are found in water samples from piezometer 7B which is about about five metres above 7C and at a higher hydraulic potential (up gradient). Unlike samples from piezometer nests 2, 4, 5 and 6, piezometer nest 7 has a higher sulphate concentration at depth.

This peculiar distribution of sulphate rich water can be explained with at least two (possibly simultaneous) scenarios. First, the screened interval in piezometer 7C appears to have intersected the southeast moving sulphate rich contamination plume which originates near the sulphur pads and runoff ponds 1, 2 and 3. Dispersion and diffusion of this plume would result in slightly elevated sulphate concentrations in the groundwater samples from 7B, this scenario is illustrated with Figure 3.4. A second explanation, which could operate concurrently with scenario one, involves the surface catchment pond 4. Water draining into this surface runoff pond has high sulphate concentrations because it originates from the sulphur dusted plant site. As shown in Figure 3.4, front view, piezometer 7B is screened at a slightly higher elevation than the surface runoff pond so that recharging water moving downward from the pond by-passes 7B.

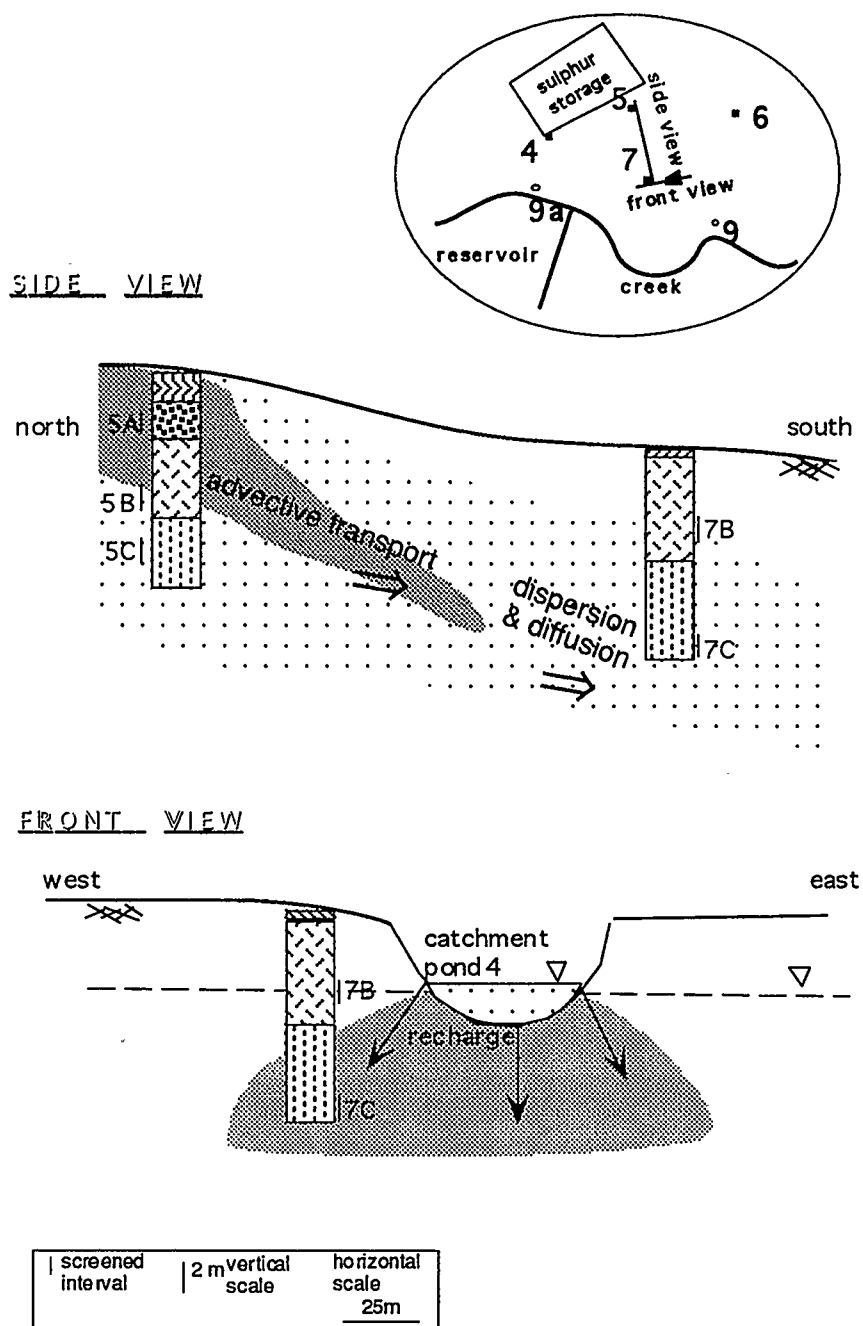


Figure 3.4: High sulphate concentrations are found in groundwater samples from 7C and not in 7B. The upper sketch is a cross-section from north to south, showing the possible movement of a sulphate rich contaminant plume. The front view illustrates catchment pond 4 as a sulphate contaminant source.

On the east side of the plant site are a series of decommissioned evaporation and sludge retention ponds. Piezometers 13N and 13S are southeast of these old ponds and the groundwater samples from 13N and 13S have sulphate concentrations as high as 1405 mg/l (w13N). During the life of the gas plant items ranging from oil waste to sulphur rich debris were deposited in the ponds. It is likely that they serve as groundwater contamination sources. Also, adjacent to the sulphur processing area and down gradient from the sludge ponds is piezometer 2A. It was not surprising to measure sulphate concentrations of 922 and 1027 mg/l in groundwater collected from this piezometer.

3.3 Calcium, Magnesium and Sodium Concentrations

Calcium and magnesium are the dominant cations in both the pristine and gas plant groundwater samples (Table 2). Calcium concentrations range from 76 mg/l (f6C) to 654 mg/l (j5A), while magnesium ranges from 28 mg/l (f#1) to 698 mg/l (f5A). The groundwater samples with high calcium concentrations vary more with the season than the low concentration waters. For example over four sampling sessions, calcium concentrations from 4C and 6C have standard deviations of 2.5 and 4.9 mg/l respectively, while 5A, 7C and 13N are 10, 38 and 41 mg/l respectively. Ion concentration fluctuations in the groundwater result from changes in infiltration, evaporation and dilution rates and/or exchange reactions.

As shown in Figure 3.6 magnesium concentrations vary little with the season. This shows that the magnesium source is less sensitive to environmental

changes than the calcium source. If dolomite [$\text{CaMg}(\text{CO}_3)_2$] dissolution is the primary source of magnesium then dissolution is expected to be slower than for calcite. Sample w5C (winter) showed the only spike in magnesium concentration. An extreme increase in the w5C magnesium (+70 mg/l) and calcium (+250 mg/l) occurs with a 600 mg/l increase in the winter sulphate concentration. The w5C Ca-Mg-SO₄ concentrations follow the linear trend illustrated in Figure 3.3.

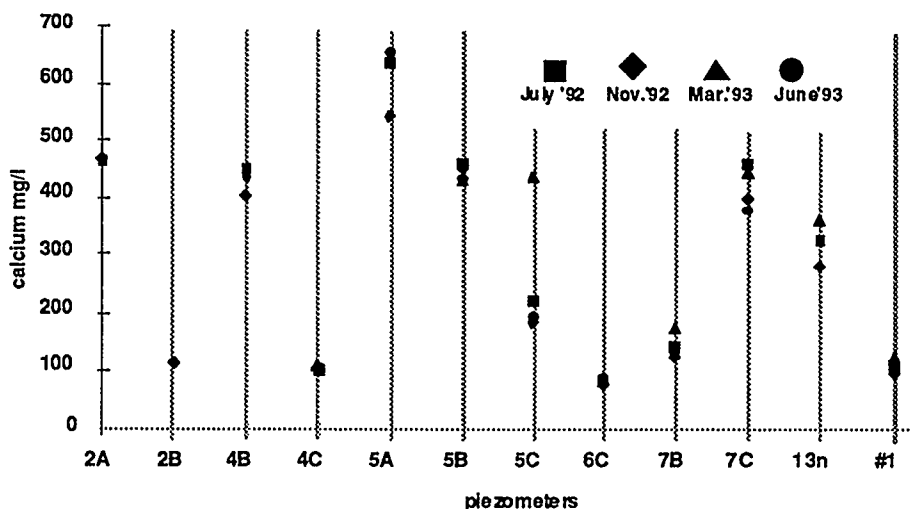


Figure 3.5: The calcium concentrations were lowest in November 1992.

Sample 13S has unusually high sodium concentrations (250 mg/l). There are several possible explanations for this anomaly. The sodium could be from an industrial source, such as the neighboring sludge pits. However, groundwater samples from piezometer 13N, which is a metre down gradient from 13S, does not have high sodium concentrations. There is no evidence for an impermeable boundary between 13N and 13S that would allow 13S groundwater

contamination in isolation of 13N. Salt (NaCl) is a common source of increased dissolved sodium concentrations in groundwater. However, there is no correlation between chloride and sodium concentrations in the 13S water samples.

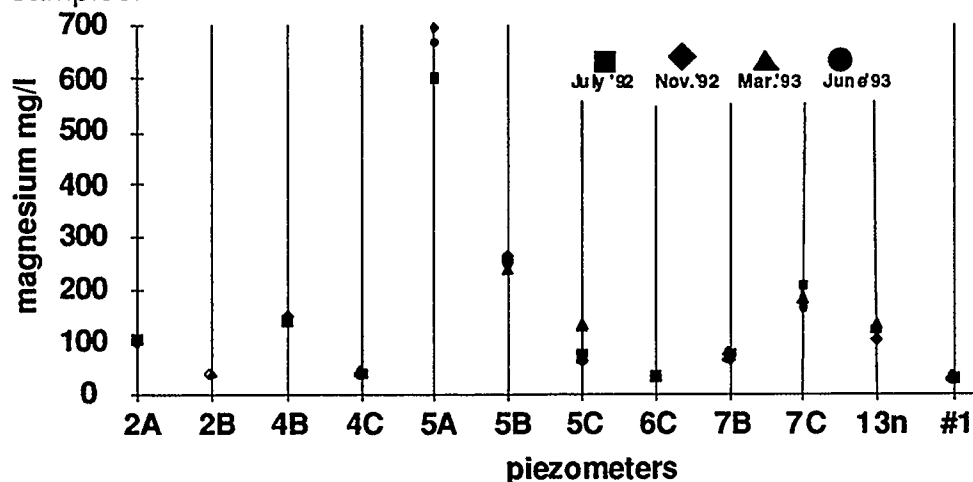


Figure 3.6: The magnesium concentration in the groundwater samples varies little through out the year.

Another possible explanation for the high sodium concentrations in 13S water samples is cation exchange. Cation exchange is a reaction in which cations within a clay mineral are replaced by cations in the surrounding solution. In the 13S example, calcium or magnesium ions in solution could be exchanging for clay bound sodium ions. The members of the clay mineral group smectite, which is common in Alberta glacial tills, is notorious for cation exchange. If exchange between a sodium smectite ($\text{Na}_{0.33}\text{Al}_2\text{Si}_4\text{OH}_2 \cdot n\text{H}_2\text{O}$) is occurring calcium or magnesium concentrations in solution should be inversely proportional to sodium concentrations in solution. As shown in Figure 3.7, this trend is not found; in fact, the calcium and sodium concentrations are positively

correlated. Magnesium concentrations vary little in all three water samples collected from 13S indicating that magnesium is not exchanging with sodium.

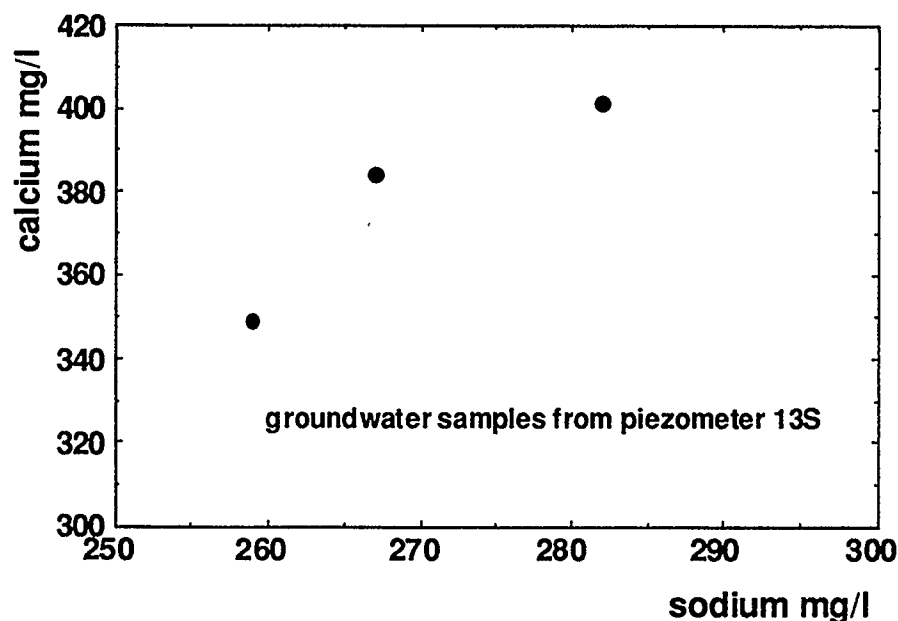


Figure 3.7: Calcium and sodium concentrations for groundwater collected from piezometer 13S have a positive correlation. The highest concentrations correspond to the lowest pH (6.52).

The confinement of high sodium concentrations to the groundwater in piezometer 13S suggests that the source or process responsible for the elevated sodium concentrations is very localized. As outlined in Figure 1.2, bentonite, a swelling clay formed from the chemical alteration of volcanic ash, is used to seal piezometer installations. Bentonite typically contains sodium rich smectites. When the interlayer cation of smectite is sodium, the amount of interlayer water accepted by the clay is almost infinite. This hydration results in

an impermeable mass which is why Na-bentonite is used for sealing. However, fissures can form in the bentonite if it has not hydrated completely. It is also possible that bentonite pellets are disintegrating at the bottom of the piezometer tube. Regardless, if acidic water attacks bentonite the sodium concentration in solution would increase. If bentonite decomposition is responsible for the increase in sodium concentration then an increase in calcium concentration due to acid reactions with carbonate minerals in the subsurface would also be expected (Figure 3.7). This is consistent with the sodium concentration high (282 mg/l) occurring with the pH low (6.52). Because ionic information from piezometer 13S is suspect, it is not included in the chemical data set.

3.4 Stable Isotopes

Ionic strength of groundwater is often an indicator of the degree of groundwater contamination. For this reason, ionic strength is compared with another potential contaminant tracer $\delta^{34}\text{S}$. As shown in Figure 3.8 an increase in ionic strength accompanies an enrichment in sulphate ^{34}S .

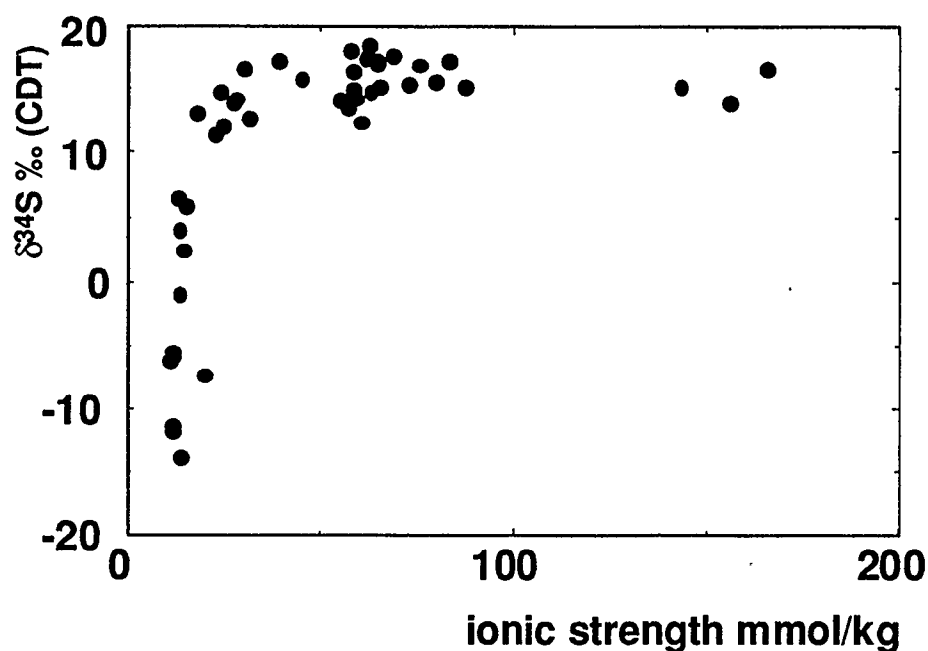


Figure 3.8: Groundwater ionic strength increases with ^{34}S enrichment.

Similarly, $\delta^{34}\text{S}$ values increase with sulphate concentration (Figure 3.9). The likeness between Figure 3.8 and 3.9 is not unexpected given Figure 3.2. Relative ^{34}S abundances range from -13.9 ‰ (spring #1) to +18.3 ‰ (w13N). The $\delta^{34}\text{S}$ for the anthropogenic sulphur source is usually +16.8 ‰ although this can vary ± 1.5 ‰. Figure 3.9 shows that as sulphate concentrations exceed background (@70 mg/l), $\delta^{34}\text{S}$ abruptly approaches that of the anthropogenic source. This can be explained by the situ-equations below:

$$(3.2) \quad (1 \text{ aliquot @ } -13\text{‰}) + (1 \text{ aliquot @ } +18\text{‰}) = (2 \text{ aliquot @ } +2.5\text{‰}) \Rightarrow$$

$$(3.3) \quad (1 \text{ aliquot @ } +2.5\text{‰}) + (1 \text{ aliquot @ } +18\text{‰}) = (2 \text{ aliquot @ } +10.3\text{‰}) \dots$$

precipitation δD , show no correlation with season or depth. The absence of strong trends in the δD data indicates that recharge from precipitation follows a complicated path that likely includes evaporation / condensation, mixing with existing groundwater and mixing with fresh precipitation. $\delta^{18}O$ variations are discussed in Chapter 5, where water/rock interactions are considered.

CHAPTER 4: $\delta^{34}\text{S}$ AS A TRACER OF ANTHROPOGENIC SULPHATE IN SHALLOW GROUNDWATER

4.1 Sulphate Reducing Bacteria

As introduced in Chapter 1, sulphate reducing bacteria (SRB) can cause a ^{34}S enrichment in sulphate due to the preferential reduction of $^{32}\text{S}^{16}\text{O}_4$. If bacterial sulphate reduction enriches the remaining groundwater sulphate in ^{34}S , elevated $\delta^{34}\text{S}$ values may not be indicative of anthropogenic sulphate and $\delta^{34}\text{S}$ would not be a conservative tracer. To appraise $\delta^{34}\text{S}$ as a tracer, measurements were made to detect the presence and/or activity of SRB's in the groundwater samples. In addition, the amount of dissolved oxygen in-situ was measured to assess the suitability of the subsurface environment for sulphate reduction. Finally, an experiment was completed to test for $\delta^{34}\text{S}$ enrichment after a seven month anoxic incubation.

$\delta^{18}\text{O}_{\text{sulphate}}$ can be a useful diagnostic tool because the exchange of O_2 atoms between sulphate and water is extremely slow (Lloyd, 1967, e.g. Hendry et al., 1986), so that the $\delta^{18}\text{O}$ of sulphate does not change after sulphate formation. Preferential reduction of $^{32}\text{S}^{16}\text{O}_4$ by bacteria should result in an enrichment of both sulphur and oxygen isotopes in the remaining sulphate. As shown in Figure 4.1, a positive correlation between $\delta^{18}\text{O}$ and $\delta^{34}\text{S}$ of the groundwater sulphates does not exist. There is a tendency for the samples with low sulphate concentrations (#1, 4C, 6C <200 mg/l) to have relatively enriched $^{18}\text{O}_{\text{sulphate}}$. This suggests that natural sulphate either incorporates oxygen from an ^{18}O -

enriched source during formation or sulphate reduction enriches the remaining sulphate in ^{18}O . The data do not allow a unique solution.

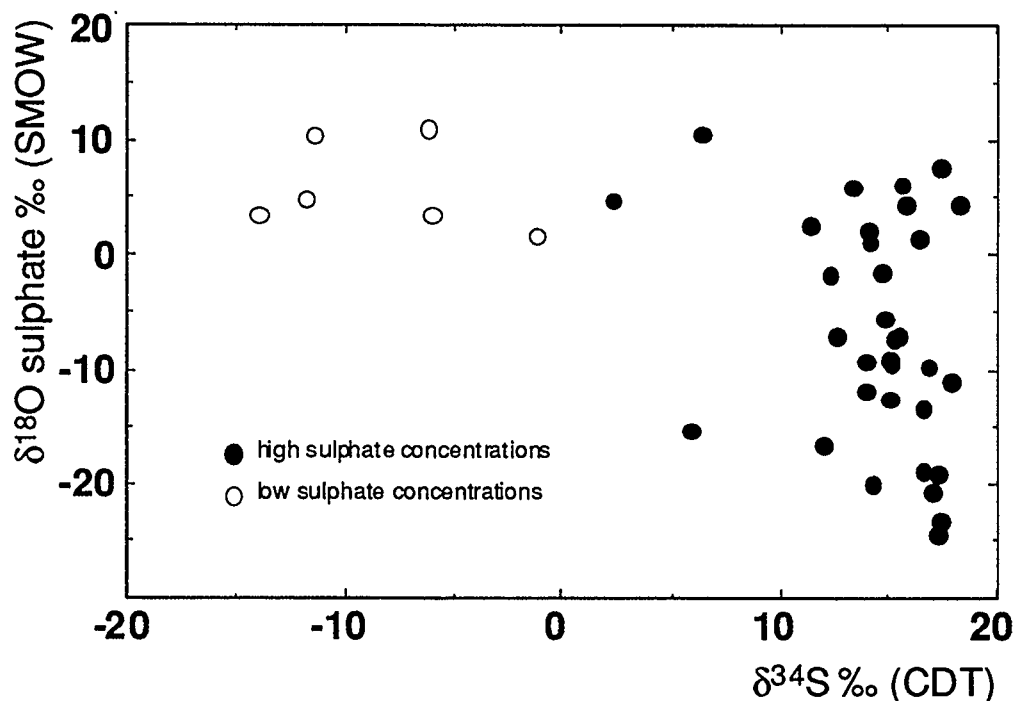


Figure 4.1: A positive correlation between $\delta^{18}\text{O}_{\text{sulphate}}$ and $\delta^{34}\text{S}_{\text{sulphate}}$ does not exist. The more pristine samples are $^{18}\text{O}_{\text{sulphate}}$ enriched.

Samples enriched in $\delta^{34}\text{S}$ have both positive (7B) and negative (5B) $\delta^{18}\text{O}_{\text{sulphate}}$ values. Negative $\delta^{18}\text{O}_{\text{sulphate}}$ values at this latitude are consistent with oxidation of sulphur compound in water with a large meteoric component (e.g. Hendry et al., 1989). Variations in $\delta^{18}\text{O}_{\text{sulphate}}$ of sulphate formed *in-situ* could reflect changes in the $\delta^{18}\text{O}$ of the groundwater. This embraces processes such as relative ^{18}O enrichment during evaporation of recharging water and

dissolution of carbonate minerals. Also, variations in $\delta^{18}\text{O}_{\text{sulphate}}$ could be due to more or less atmospheric oxygen ($\delta^{18}\text{O} = +23 \text{‰}$) incorporation in the sulphate.

It was hypothesized that under aerobic conditions bacteria that use O_2 dissolved in water will dominate over the SRB's that use oxygen from dissolved sulphate. Concentrations of O_2 in the groundwater were measured downhole during the March 1993 and June 1993 samplings. The results are listed in Table 2. As shown, O_2 is present in concentrations that range from 0.6 to 3.9 mg/l. Under these aerobic conditions it is expected that bacteria that use dissolved oxygen will dominate over SRB's (e.g. Hendry et al., 1986).

Tests for the hydrogenase enzyme (Bryant et al., 1991) showed two of the samples (w5B, w6C) to be moderately positive (level 2), two (w5C, w4C) weakly positive (level 1) and three of the samples (w7B, w7C, w13s) tested negative. Based on this test, there is a 95% probability that active SRB's are present in sample w5B and w6C.

The presence of SRB's *per se* does not imply that ^{34}S enrichment occurs in unreacted sulphate during transport from the water table to the piezometer screens. The objective of the incubation experiment was to test for $\delta^{34}\text{S}_{\text{sulphate}}$ shifts under anoxic conditions over a period of time consistent with hydrogeologic information. In the hydrogeologic model (section 2.3), recharging groundwater reaches the sampling screens in approximately 2 days to 5 years.

To test the extreme case, a completely anoxic incubation of groundwater samples was carried out. Three filtered (0.45 μ m) and five unfiltered 120 ml aliquots of groundwater from November 1992 were sealed for seven months at 25°C. Unfiltered waters should contain host substrate for bacteria and more organic material (soil debris, food energy for bacteria and/or organisms) than filtered water samples. This incubation test is tough because the samples were not exposed to atmospheric O₂.

As shown in Table 4, the $\delta^{34}\text{S}$ shifts upon incubation were very small even under anaerobic conditions. Therefore, it is highly unlikely that significant shifts occur during transport in cooler water with dissolved O₂. The differences between the samples ($\pm 1\text{‰}$) can be attributed to variations in the measurements. Hendry et al. (1986) found $\delta^{34}\text{S}$ varied $\pm 0.5\text{‰}$ using the same instrument. Norman (1991) measured a standard deviation as high as 1.5‰ on small samples (<0.4 mg SO₄).

TABLE 4: $\delta^{34}\text{S}$ of incubated November 1992 samples

sample	$\delta^{34}\text{S}$	$\delta^{34}\text{S}$	$\delta^{34}\text{S}$
	‰ CDT	‰ CDT	‰ CDT
	<i>original</i>	<i>incubated filtered</i>	<i>incubated not filtered</i>
5A	14.0	15.0	14.7
5B	15.1	--	15.2
7B	13.1	14.8	13.6
7C	15.1	--	15.6
13N	15.8	15.8	15.8

4.2 Anthropogenic Sulphate Identified with $\delta^{34}\text{S}$

The $\delta^{34}\text{S}$ values of groundwater sulphate appear to behave conservatively so that it is possible to distinguish between anthropogenic and natural sulphate. Figure 3.8 illustrates how ^{34}S enrichment corresponds to an increase in sulphate concentration. With one exception (f2B), for sulphate concentrations above 50 mg/l, the $\delta^{34}\text{S}$ values have a mean of 15.2 ‰ corresponding to a dominance of industrial sulphate. At lower concentrations the $\delta^{34}\text{S}$ approaches that of spring #1. The dominance of anthropogenic sulphate is illustrated by a negatively skewed distribution of $\delta^{34}\text{S}$ values (Figure 4.2).

Spring #1, which was selected earlier as the geochemical background sample, also serves as the background $\delta^{34}\text{S}$ sample. At the bottom of Table 2 the range

of $\delta^{34}\text{S}$ for spring #1 (-11.4 ‰ to -13.9 ‰) is typical for natural aqueous groundwater sulphate.

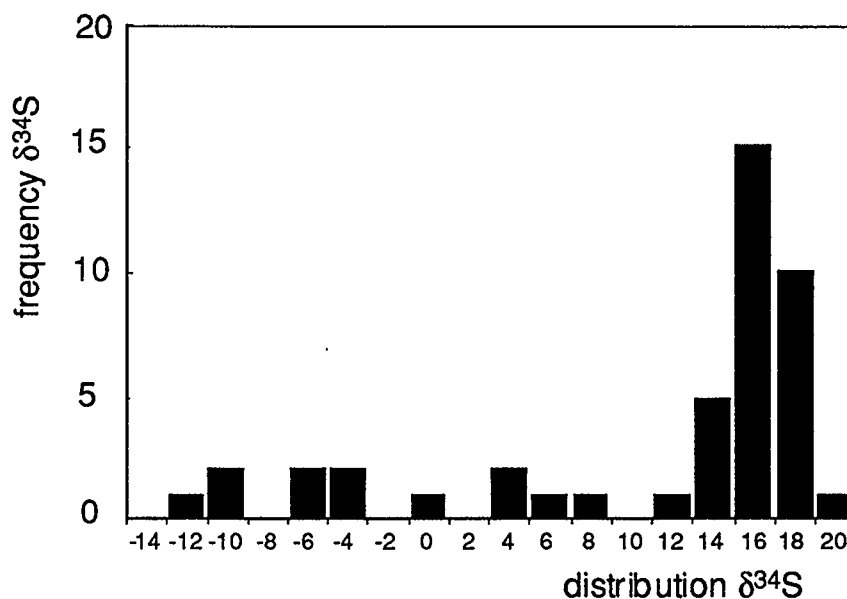


Figure 4.2: The distribution of $\delta^{34}\text{S}$ data shows that a majority of the aqueous sulphate samples contain anthropogenic sulphate.

Figure 4.3 shows the June 1993 $\delta^{34}\text{S}$ in cross-section. Industrial sulphate movement is defined in the vertical plane using this $\delta^{34}\text{S}$ data. The $\delta^{34}\text{S}$ tracer is very sensitive to changes in anthropogenic contribution.

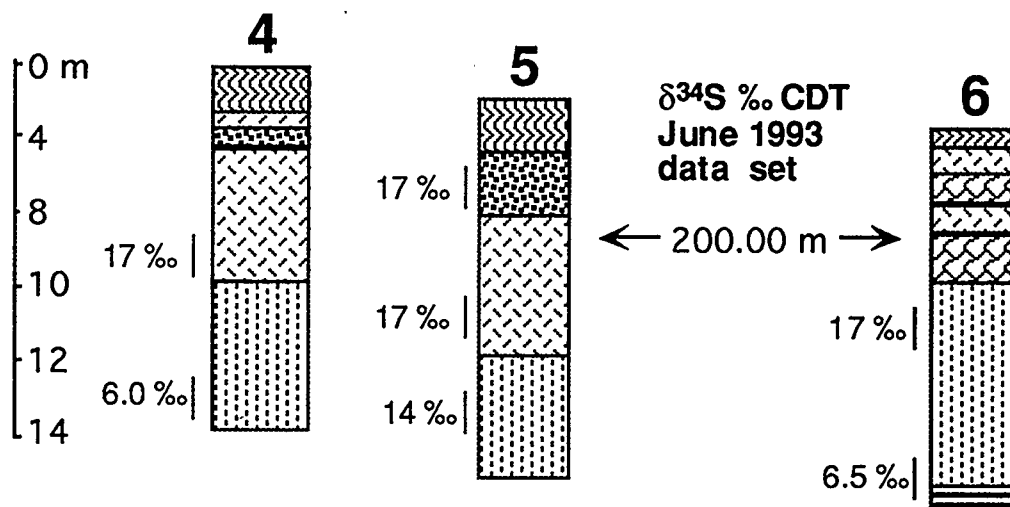


Figure 4.3: $\delta^{34}\text{S}$ values from the June 1993 data set decrease with depth. $\delta^{34}\text{S}$ values help to constrain movement of the industrial sulphate plume. Lithology types are defined in Figure 2.3.

Vertical gradients appear to be related to $\delta^{34}\text{S}$ values in groundwater sulphate from piezometers nests 4 and 7. In Figure 4.4, the difference between 7B and 7C $\delta^{34}\text{S}$ increases with the vertical gradient. This implies that increases in vertical gradient improve the vertical transport of industrial sulphate from the catchment pond adjacent to nest 7 to piezometer 7C (by-passing 7B). Of course the highest vertical gradient coincides with the wettest month (June), this precipitation would tend to fill catchment pond 4 with sulphate rich water from the plant site.

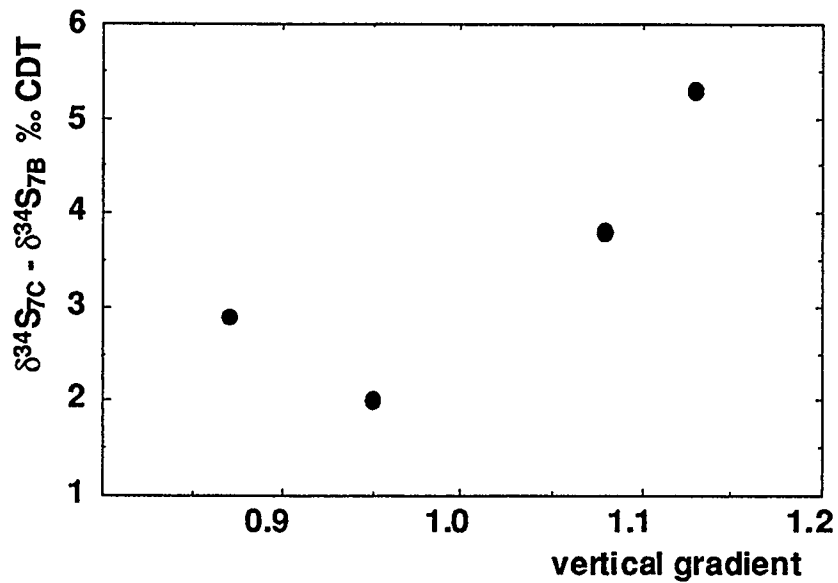


Figure 4.4: The difference in $\delta^{34}\text{S}$ values for 7B and 7C increase with the vertical gradient.

The opposite relation is found in piezometer nest 4 because, unlike nest 7, the ^{34}S rich source does not by-pass the upper sample point. An increase in vertical hydraulic gradient appears to enhance mixing between the upper sulphate contaminated zone (4B) and the lower more pristine groundwater (4C) so that the difference in $\delta^{34}\text{S}$ values decreases.

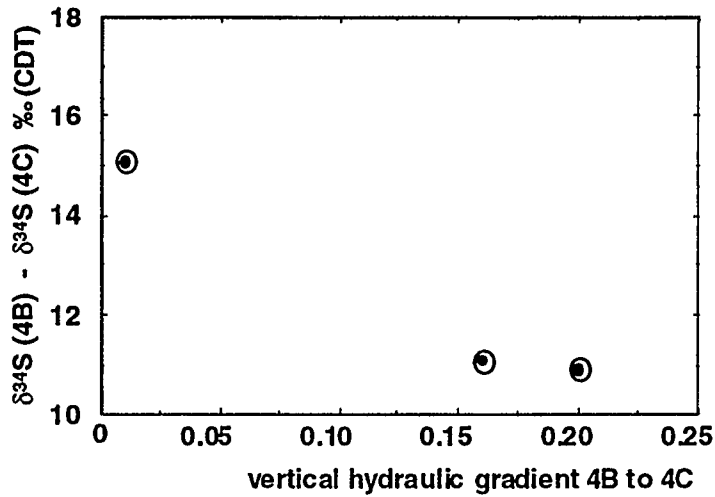


Figure 4.5: As the vertical gradient increases between 4B and 4C the difference between groundwater sulphate $\delta^{34}\text{S}$ decreases.

In a system where there are only two sulphate sources, a fixed source and a variable one, the $\delta^{34}\text{S}$ values and sulphate concentrations can be used to identify the variable source. If it is assumed that only two main $\delta^{34}\text{S}$ end members exist, then a plot of $\delta^{34}\text{S}$ as a function of $[\text{SO}_4]^{-1}$ will have a y-intercept equal to the variable source. This relation is described by the following series of equations:

$$(4.1) \quad C\delta = C_a\delta_a + C_b\delta_b$$

$$(4.2) \quad C = C_a + C_b$$

$$(4.3) \quad \delta = C_a(\delta_a - \delta_b) \cdot (C)^{-1} + \delta_b$$

where: C_a, C_b = the concentrations of sources a & b
 δ_a, δ_b = the $\delta^{34}\text{S}$ values of sources a & b
 C, δ = the concentration & $\delta^{34}\text{S}$ measured,

For a mixture of a and b, a plot of δ versus $[C]^{-1}$ will yield a y-intercept equal to δ_b (Krouse, 1980). In this study, $[C] = [SO_4]$ and δ_b (the variable source).

The regression line in Figure 4.6, has a y-intercept (δ_b) $\delta^{34}S \cong +16.2\text{‰}$ and a correlation coefficient of -0.81, which identifies the gas plant as the dominant variable source. It is possible that the background source is slightly variable in concentration and that background aqueous sulphate originates from many organic and inorganic natural sources. Also, because the concentration of the industrial source (gas plant) is not highly variable the regression line is not well constrained. The precipitation sample does not fall on the line because roughly the entire source of sulphate measured in the rain sample is from the gas plant. There is very little natural sulphate in rainfall in the region (Hendry et al. , 1986). Oddly, sample f2B does not follow the trend. The f2B groundwater sample has a high concentration of sulphate (334 mg/l) and is depleted in ^{34}S . The sulphate in this sample could be from another natural source. This anomalous data point is difficult to clarify because it is the only sample collected from piezometer 2B.

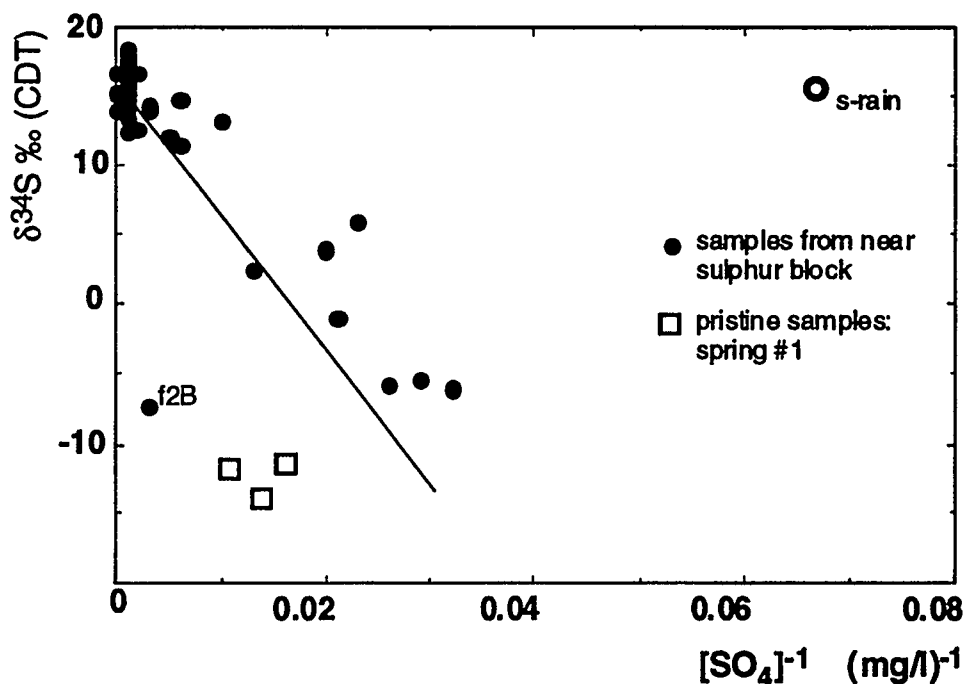


Figure 4.6: The y-intercept of the linear regression line in this plot ($\delta^{34}\text{S} \cong +16$ ‰) identifies the gas plant as the dominant variable source of sulphate.

Two main criteria are met at this site which allow $\delta^{34}\text{S}$ to work as an effective tracer of anthropogenic sulphate in groundwater. First, the difference between natural and anthropogenic sulphate $\delta^{34}\text{S}$ is large. Second, the activity of sulphate reducing bacteria does not result in ^{34}S enrichment of the remaining sulphate. The low activity of SRB's at this site is probably related to the presence of O_2 in the groundwater (mean 2 mg/l).

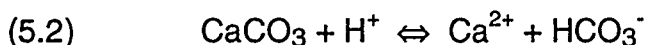
CHAPTER 5: ALTERATION OF GROUNDWATER CHEMISTRY BY SULPHATE

5.1 Introduction of Sulphuric Acid

The high industrial sulphate concentrations acidify the recharge water (reaction 5.1) and change the chemistry of the groundwater by reacting with minerals in the glacial till.



Discharge from the surface runoff pond 1, next to piezometer nest 5, has a pH of 1.9 (November, 1992). Remarkably, the pH of the shallow groundwaters surrounding the sulphur pads are near neutral. In contrast to the acidic sulphate problems of eastern Canada (e.g. Nriagu et al., 1983), the pH of these waters are independent of sulphate concentration. Ionic and isotopic evidence suggest that calcite (CaCO_3) dissolution and/or to a lesser extent the dissolution of other minerals are buffering the H^+ activity (reaction 5.2).



5.2 Geochemical Evidence of Acid Buffering by Minerals in Glacial Till

Evidence from aqueous chemistry for reactions 5.1 and 5.2 is found in the near-linear relationship between elevated calcium and sulphate concentrations,

Figure 5.1. At higher sulphate concentrations the calcium concentrations tend to level off suggesting that a calcium sink exists. The precipitation of calcium bearing minerals, such as gypsum, could produce this effect.

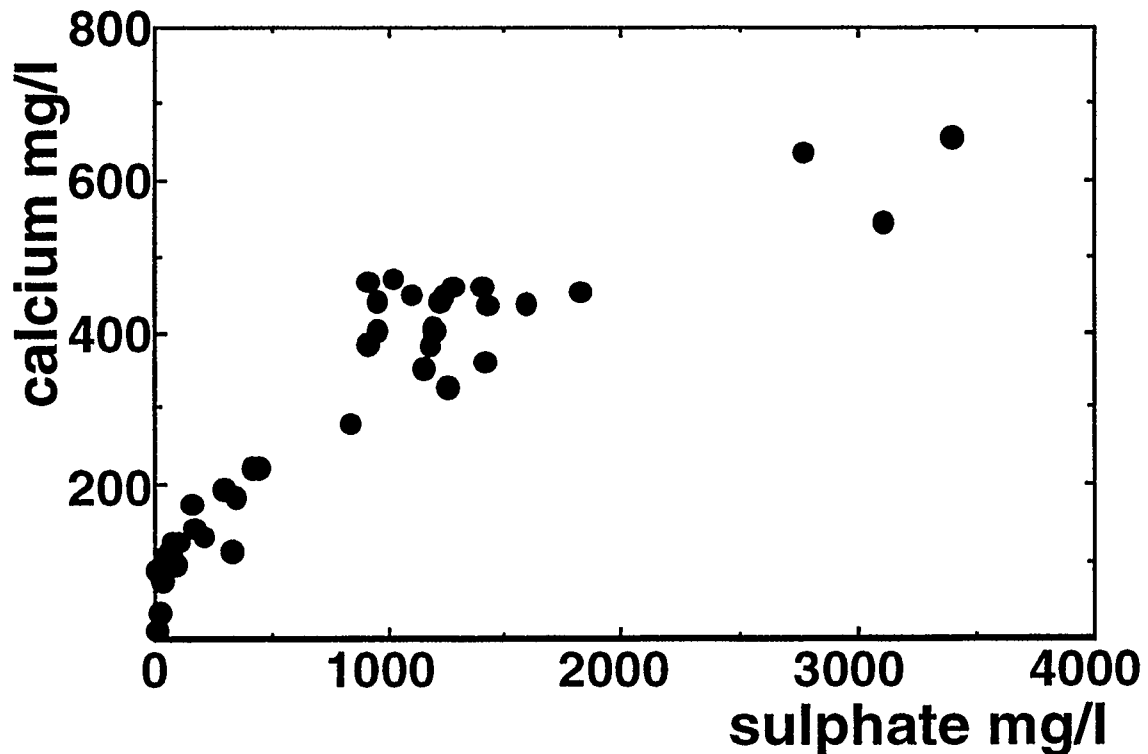


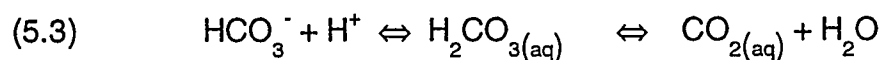
Figure 5.1: Calcium concentrations are strongly correlated with sulphate concentrations (correlation coefficient for linear regression = 0.84), suggesting that excess H^+ is attacking calcite.

Potassium, sodium, iron and manganese also increased in concentration in the more sulphate-rich waters, suggesting that minerals other than calcite and dolomite are altered by sulphuric acid.

Further indications that carbonate mineral dissolution is occurring were found using a mineral speciation model (SOLVEQ by Reed and Spycher, 1989). All of

the groundwater samples are either under saturated or slightly saturated with respect to calcite. Calcite saturation is predicted for both high ionic strength water samples (e.g. j5A) and low ionic strength waters (e.g. w#1). In the waters undersaturated with respect to calcite, dissolution is probably occurring.

A relation between sulphate concentration and alkalinity was anticipated because of reaction 5.2. There is a tendency for alkalinity to increase with sulphate concentration (Figure 5.2). The relation is feeble presumably because variable amounts of HCO_3^- transform to CO_2 (g) which escapes to the atmosphere (reaction 5.3) or because there are other sources of CO_2 (g) in the subsurface.



Under atmospheric conditions, in the piezometer tube, the CO_2 (aq) will tend to CO_2 (g). The partial pressure of CO_2 ($p\text{CO}_2$) is less in the piezometer tube than in the subsurface where CO_2 is generated by plant decay, mineral / water interactions and bacterial activity (Domenico and Schwartz, 1990).

There is also physical evidence that calcite is not in equilibrium with the groundwater and that dissolution and precipitation are occurring. Calcite precipitate is found near the discharge points of spring #9b and pristine spring #1. This discharging groundwater, rich in calcium and bicarbonate, is responding to the relative drop in $p\text{CO}_2$, which drives reaction 5.3 and 5.2 to the left forcing precipitation of CaCO_3 .

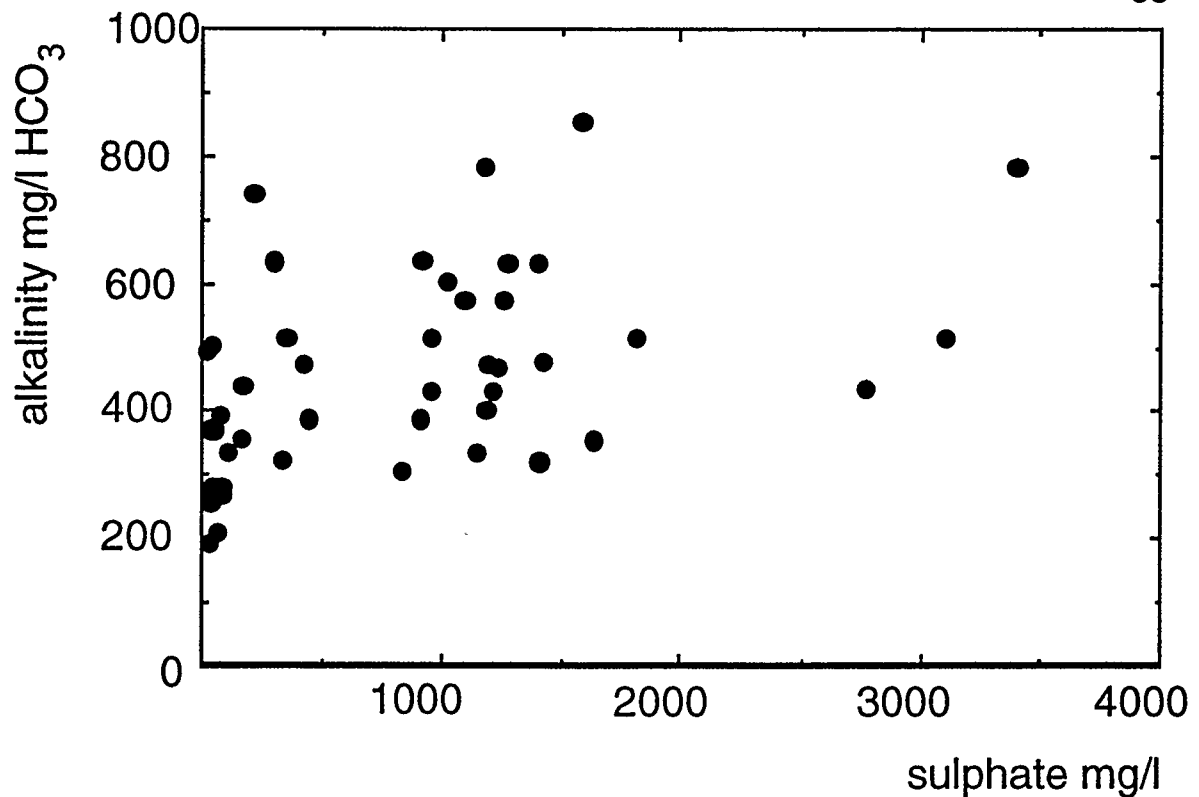


Figure 5.2: Alkalinity and sulphate concentration tend to increase with each other.

It is likely that other minerals besides carbonates are influencing groundwater chemistry. Because the glacial till at this site has a large clay component (Figure 2.3) the possibility of a Ca-Mg rich clay effecting ion concentrations was investigated using a phase diagram. If ion activities cluster close to a mineral phase boundary it suggests that the water chemistry is in equilibrium with the mineral reaction delineated by the phase boundary (Hutcheon, per.com. 1993). The relation between calcium and magnesium activities and Ca-Mg beidellite was investigated because the groundwater samples at the study site are calcium and magnesium rich. Beidellite is a dioctahedral smectite which has magnesium and calcium end members. Smectite is common in Alberta glacial

till deposits and was identified in soil samples from the plant site area using XRD clay separate techniques.

The Mg-Ca beidellite phase boundary shown in Figure 5.3 was constructed using a computer program, PTA (Brown et al., 1988). The Mg and Ca beidellite activities needed for PTA were calculated from a pristine groundwater analysis (f#1) using thermodynamic data compiled by Abercrombie (1989). The magnesium and calcium activities for the groundwater samples were estimated using SOLVEQ (Reed and Spycher, 1989). The activity information was superimposed on the phase diagram. As shown in Figure 5.3, a majority of the groundwater samples cluster along the Ca-Mg beidellite phase boundary suggesting that the water chemistry is in equilibrium with beidellite.

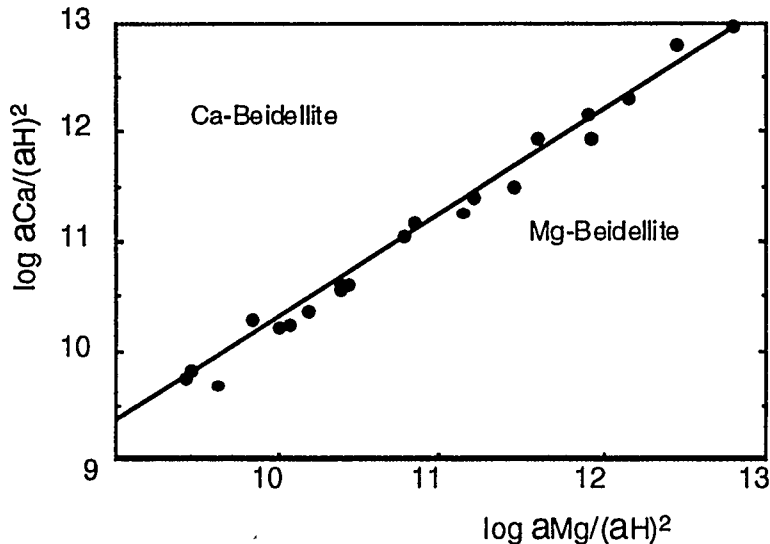


Figure 5.3: The activity quotients of $\log(aCa/aH^2)$ and $\log(aMg/aH^2)$ cluster along the equilibrium line for Ca-Mg beidellite. The phase boundary uses Mg and Ca beidellite activities which are assumed to be in equilibrium with pristine groundwater (sample f#1).

5.3 Isotopic Evidence of Ancient Carbonates In Glacial Tillis as an Acid Buffer

Isotopic indications of carbonate mineral dissolution are found on the δD versus $\delta^{18}O$ graph, Figure 5.4. Enrichment of ^{18}O relative to the meteoric line is often due to oxygen exchange between recharging waters and dissolving rock minerals (e.g. Fontes, 1980).

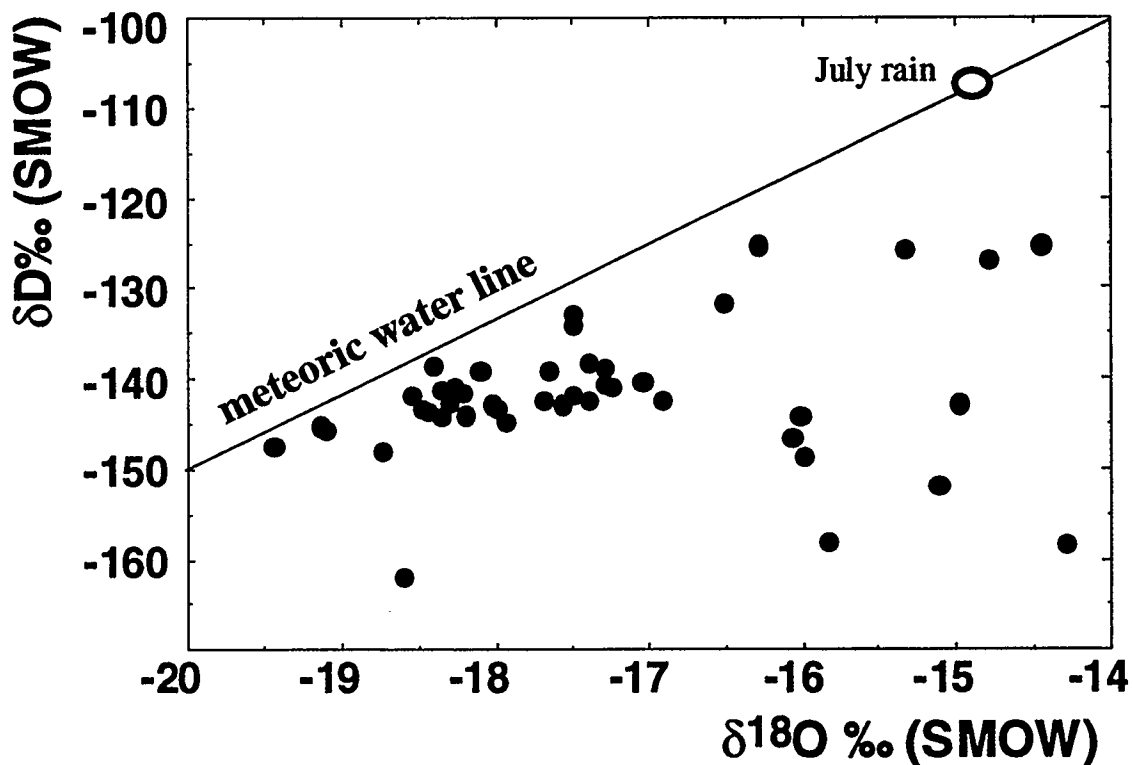


Figure 5.4: The relative enrichment in ^{18}O of the groundwater shifts the data points away from the meteoric line.

Groundwater becomes enriched in ^{18}O when carbonate rock fragments (e.g. limestone, dolomite) dissolve because the oxygen contained in these minerals is ^{18}O enriched. O_2 equilibrium between HCO_3 and H_2O is fast, therefore,

dissolved carbonate species from ancient marine carbonates will enrich the ^{18}O of the groundwater. The isotopic evidence for calcite dissolution and acid buffering in the groundwater centres around this hypothesis.

By reaction 5.2, increases in calcium should accompany enrichment in groundwater ^{18}O . As shown in Figure 5.5 the two appear to be related; an increase in calcium concentrations corresponds to an enrichment in ^{18}O . Rain water, which has not interacted with any minerals, does not follow the trend.

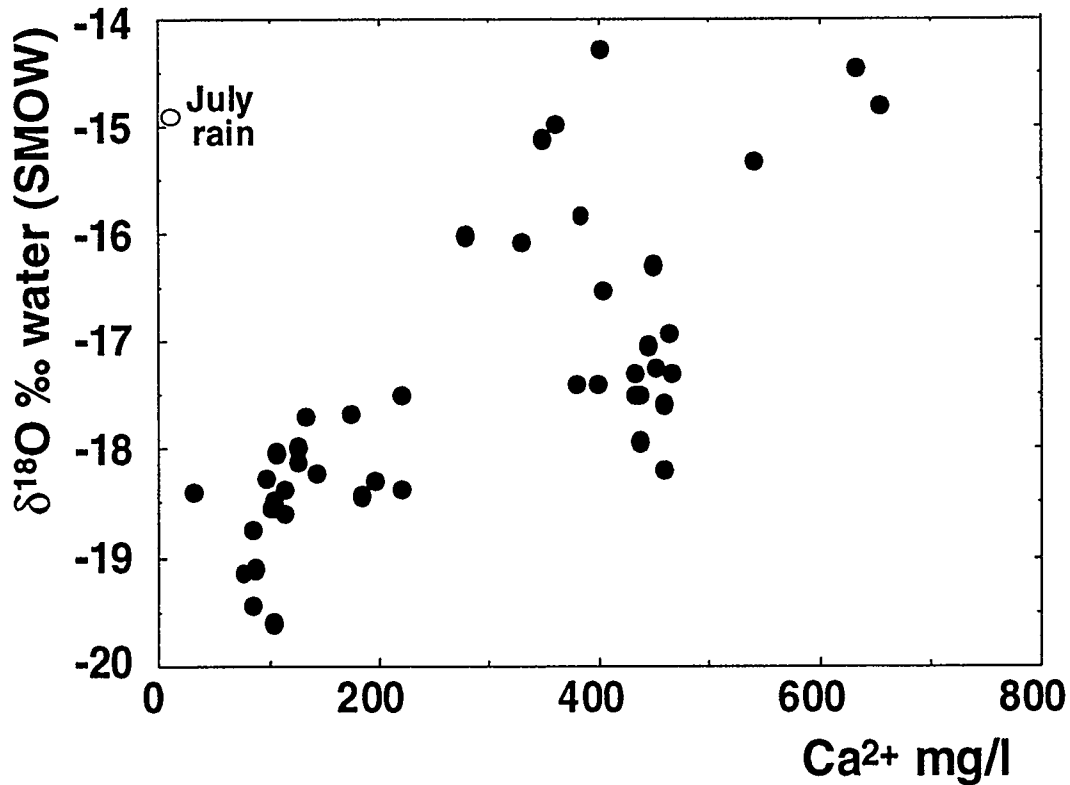


Figure 5.5: $\delta^{18}\text{O}$ (water) and calcium concentration appear to be related,, as CaCO_3 (calcite) dissolves, the groundwater becomes enriched in $\delta^{18}\text{O}$. Summer rain water does not follow the trend.

The relationship between $\delta^{18}\text{O}$ and $[\text{Ca}^{2+}]$ would be stronger if CaCO_3 was the only source of calcium and if ions in solution were not mobile. The decomposition of other calcium bearing minerals such as anorthite (plagioclase feldspar end member) and/or calcium bearing clays may also contribute to the calcium pool. A plot of $\delta^{18}\text{O}$ versus HCO_3^- is shown Figure 5.6. An enrichment in ^{18}O with increasing HCO_3^- concentration was anticipated due to equation 5.2. However, the relation is not strong for reasons similar to Figure 5.2 (alkalinity and sulphate concentrations).

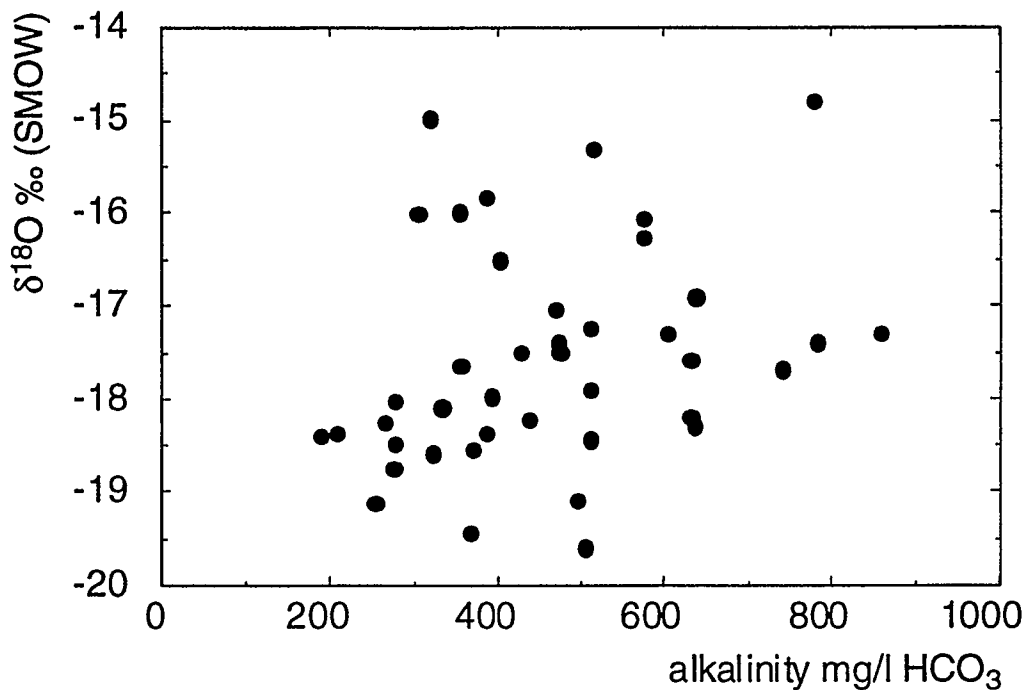


Figure 5.6: $\delta^{18}\text{O}$ of the groundwater is somewhat higher in the more alkaline water samples.

The magnitude of the $\delta^{18}\text{O}$ shift away from the meteoric water line (Figure 5.4) should be proportional to the contact time between the infiltrating water and the minerals. It is difficult to determine if contact time is a significant variable

because it requires accurate knowledge of the vertical transport time for each sample point. Also, as suggested by the $\delta^{18}\text{O}$ and high calcium and sulphate concentrations from piezometer 5A, geochemical alteration in the vadose zone is significant. Finally, ^{18}O enrichment in the groundwater will be affected by the season (relative winter depletion) and evaporation / condensation.

5.4 Gypsum Precipitation in Sulphate Contaminated Groundwater

The high concentrations of calcium and sulphate in the groundwater samples leads to the question: is gypsum ($\text{CaSO}_4 \cdot 2\text{H}_2\text{O}$) precipitation occurring in the subsurface? To investigate this question the saturation indices of the groundwater samples were calculated using SOLVEQ (Reed and Spycher, 1989).

The following short digression is presented to explain saturation indices and provide an example from the groundwater data set. The saturation index (S.I.) gives an indication of how close a mineral is to equilibrium with ions in a solution. It is the ratio of the reaction quotient (Q) to the equilibrium constant (K_{eq}) of a particular mineral. Q comes from the law of mass action:

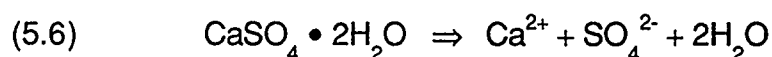


where b, c, d, e are the number of moles of the chemical constituents B, C, D, E. The reaction quotient is the ratio of the products to the reactants:

$$(5.5) \quad Q = [D]^d [E]^e / [B]^b [C]^c$$

where [B], [C], [D] and [E] are activities, or the thermodynamically effective concentration of a species. Reaction 5.4 proceeds either right or left in order to achieve an equilibrium condition. At equilibrium, the equilibrium constant (K_{eq}) equals the quotient shown in (5.5). K_{eq} can be calculated from free energy (ΔG_R) data. Therefore, for a particular mineral, if Q equals K_{eq} then the solution is at equilibrium with respect to that mineral. If S.I. is less than 1 then mineral dissolution should occur (equation 5.4 proceeds right) and if S.I. is greater than 1 then mineral precipitation is required to reach equilibrium. Often S.I. is presented in \log_{10} notation so that a negative log S.I. is under saturated, a positive log S.I. is super saturated and $\log S.I. = 0$ represents equilibrium.

As an example consider reaction 5.6 for gypsum dissolution,



$$(5.7) \quad Q = [\text{Ca}^{2+}] \cdot [\text{SO}_4^{2-}] \cdot [\text{H}_2\text{O}]^2 / [\text{CaSO}_4 \cdot 2\text{H}_2\text{O}]$$

This reaction simplifies because the activity of solids (standard state) is 1, also in dilute solution the activity of water equals 1.

$$(5.8) \quad Q = [\text{Ca}^{2+}] \cdot [\text{SO}_4^{2-}].$$

Now consider a water sample from piezometer 5B (w5B) which has the following activities: $[\text{Ca}^{2+}] = 0.003585$ and $[\text{SO}_4^{2-}] = 0.00449$ (from SOLVEQ), and knowing that K_{eq} for gypsum at 7°C is approximately $10^{-4.58}$ (Drever, 1988) then the S.I. is:

$$(5.9) \quad \text{S.I.} = 10^{-4.79} / 10^{-4.58} = 0.62$$

$$\text{or:} \quad \log \text{S.I.} = -0.21$$

The groundwater sample from w5B is under saturated with respect to gypsum.

In Figure 5.7 the saturation indices are plotted in \log_{10} notation so that 0 corresponds to gypsum saturation. As shown, SOLVEQ predicts that most of the samples are very close to gypsum saturation. Also, the S.I. is displayed in Figure 5.7 as a function of $\delta^{34}\text{S}$. The increase in S.I. with ^{34}S enrichment of the sulphate confirms that anthropogenic sulphate is responsible for the increase in gypsum saturation indices. Because the $\delta^{34}\text{S}$ and $\delta^{18}\text{O}$ fractionation associated with gypsum precipitation is small, $\leq +3\text{‰}$ and $+1\text{‰}$ respectively, and because the sulphate pool is large, changes in $\delta^{34}\text{S}$ and $\delta^{18}\text{O}$ due to gypsum precipitation are insignificant (e.g. Hoefs, 1973, Krouse, 1987b).

The computer speciation model shows that many of the groundwater samples are close to gypsum saturation. To investigate the possibility of gypsum precipitation further, a small soil investigation was undertaken. The objectives of this soil investigation are:

- (1) to establish if gypsum is present in the clayey soil within the study area (sample points shown in Figure 2.2),
- (2) to investigate the origin of soluble and insoluble sulphur species within this soil.

2 m and three samples at various depths were collected from each pit. Table 5 and Figure 5.8 summarize the results.

Gypsum ($\text{CaSO}_4 \cdot 2\text{H}_2\text{O}$) was detected in the two shallow samples (1.1, 2.1) and the two deep samples (1.3, 2.3). There are no gypsum XRD peaks present in samples 1.2 and 2.2.

The $\delta^{34}\text{S}$ of the soluble sulphur fraction in all of the samples varies less than 0.5 ‰. This ^{34}S enrichment in soluble sulphur extractions confirms that the soluble sulphur species originate from the oxidation of anthropogenic sulphur. The $\delta^{18}\text{O}_{\text{sulphate}}$ data for these sulphate samples indicates that the oxygen incorporated in the sulphate is a combination of local precipitation ($\delta^{18}\text{O} \cong -18$ ‰) and atmospheric oxygen ($\delta^{18}\text{O} = +23$ ‰). If the soluble sulphur fraction originated from ancient marine gypsum dissolution the $\delta^{18}\text{O}_{\text{sulphate}}$ would be more enriched $\cong +9.5$ ‰ (e.g. Leone et al., 1987).

Unlike the soluble sulphur fraction, the insoluble sulphur $\delta^{34}\text{S}$ varies with depth. In the shallow samples, 1.1 and 2.1, $\delta^{34}\text{S}$ is similar to the anthropogenic source. The appearance (yellowish) and smell (rotten egg) of the soil, combined with the enriched $\delta^{34}\text{S}$ values of the sulphur samples, verify that the shallow insoluble sulphur portion are predominantly windblown elemental sulphur particulates from the sulphur block. The possibility of elemental sulphur from the nearby sulphur storage being incorporated into the shallow soil (0 to 15 cm depth) was not unexpected as windblown sulphur particles coat the plant site area with a yellow dust.

Insoluble sulphur samples 1.2 and 2.2 both show a depletion in ^{34}S . This suggests that ^{32}S is being preferentially incorporated into an insoluble sulphur form. Sulphate reduction could cause this depletion, however, because sulphate reduction typically occurs under anoxic conditions the possibility of sulphate reduction in this organic poor, near surface material is doubtful. Another possibility is that the insoluble form is carbon bonded sulphur. However, the difference (-6.5 ‰ sample 2.2) is quite large for carbon bonding of sulphur species. The ^{34}S depletion of these insoluble sulphur samples corresponds with an absence of gypsum, supporting the notion of that sulphate (in gypsum) is transforming into insoluble forms. In addition, sample 2.2 shows a decrease in the soluble sulphate in the soil at this depth.

The deeper insoluble sulphur samples, 1.3 and 2.3, do not have the ^{34}S depletion found in 1.2 and 2.2. The reason for the ^{34}S enrichment is not clear. It is possible that the processes which cause ^{34}S depletion in samples 1.2 and 2.2 do not occur at depth. It is also possible that the soil residue, used in the laboratory extraction of insoluble sulphur for 1.3 and 2.3, still contained ^{34}S rich soluble sulphur species.

Also of note is the increase in total sulphur with depth. In particular sample 1.3 shows a dramatic change in the mg/g of total sulphur in the soil. Because the sulphate concentration in pit #1 decreases with depth, it is assumed that the increase in total sulphur is due to increases in insoluble sulphur species.

The preceding investigation demonstrates that soil sulphur transformations can be very complicated. The XRD analysis confirms that recent gypsum

precipitation is occurring at shallow depths at the study site. Evidence for recent gypsum deposition includes $\delta^{34}\text{S}$ values very close to those of the gas plant and relatively depleted $\delta^{18}\text{O}_{\text{sulphate}}$ values. The soluble sulphur extracted from the soil accounts for less than half the total sulphur in the soil samples; therefore, a majority of the sulphur occurs in insoluble form. The changes in the insoluble sulphur $\delta^{34}\text{S}$ values suggest that isotope fractionation between soluble and insoluble sulphur forms takes place at shallow depths.

TABLE 5: SOIL INVESTIGATION SUMMARY

SAMPLE \Rightarrow	1.1	1.2	1.3	2.1	2.2	2.3
depth of sample (cm)	15	30	90	15	60	200
$\delta^{34}\text{S}$ soluble SO_4^{2-} ‰CDT	17.6	17.9	17.7	17.8	17.9	18.0
$\delta^{18}\text{O}$ of soluble ‰SMOW	-10.8	-12.5	-12.6	-10.6	-9.91	-9.95
$\delta^{34}\text{S}$ insoluble S ‰CDT	16.3	14.9	18.3	18.1	11.4	17.8
total sulphur from XRF (S mg/g soil)	9.4	4.30	24.0	11.4	0.76	5.53
SO_4^{2-} estimate mg SO_4^{2-} /g soil	4.1	3.2	1.1	.93	.4	.94
XRD summary						
% CaCO_3 (calcite)	2	4	3	11	8	4
% $\text{CaSO}_4 \cdot 2\text{H}_2\text{O}$ (gypsum)	10		10	6		7
% clay	3	5	4	2	10	4
% feldspars	24	6		7	5	19
% SiO_2	61	88	53	74	67	66

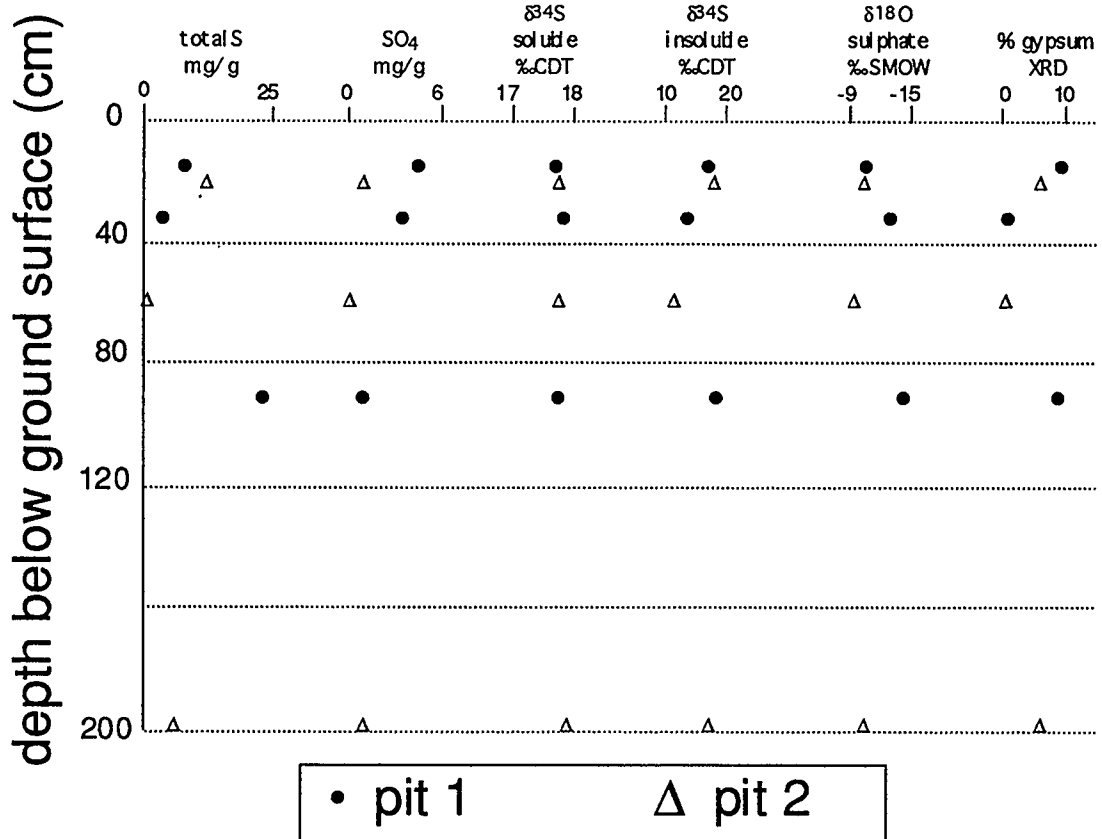


Figure 5.8: This cross-section shows variation in $\delta^{34}\text{S}$, sulphur concentration and gypsum with depth.

CHAPTER 6: CONCLUSIONS

Sulphate formed from the oxidation of anthropogenic sulphur compounds has been successfully traced in groundwater using $\delta^{34}\text{S}$. The $\delta^{34}\text{S}$ of groundwater sulphate varies with sulphate concentration which in turn depends on the season. The $\delta^{34}\text{S}$ tracer is effective at this site because of the large difference between natural and anthropogenic $\delta^{34}\text{S}$ and because the low SRB activity assures that the $\delta^{34}\text{S}$ tracer remains conservative. Sulphate reducers are not extremely active in the groundwater because the water is oxygenated (mean dissolved oxygen 2.0 mg/l).

The location of the sour gas plant, on top of a hill bounded by creeks, strongly affects the direction of groundwater flow and advective transport of industrial sulphate. Groundwater recharges on top of the hill, moves downward through glacial material, and south east towards the creek banks where it discharges along the glacial / bedrock contact. Because groundwater recharge is occurring at the plant site elemental sulphur is leached downward into the groundwater system.

Considerable chemical alteration of groundwater occurs along the flow path due to reactions between minerals present in the glacial till and the acidic (H_2SO_4) recharging water. In particular, carbonate minerals in the glacial overburden significantly affect the contaminated groundwater chemistry. Because of the pH buffering associated with these reactions, recharging water with a pH of 2 returns to a pH near 7 within several metres of the ground surface. This carbonate mineral buffering process is inferred from a positive

correlation between calcium and sulphate concentrations as well as magnesium and sulphate concentrations. In addition, the ^{18}O enrichment of groundwater samples verifies that ^{18}O rich carbonate material is dissolving. A weak, yet positive correlation exists between $\delta^{18}\text{O}$ values of the groundwater calcium, sulphate and bicarbonate concentrations. A geochemical speciation model (SOLVEQ) supports the notion of calcite dissolution by predicting calcite under saturation in most cases. Finally, the presence of calcite tufa at spring discharges near the gas plant provides further support for the "calcite as a pH buffer" hypothesis.

Precipitation of gypsum is anticipated in the groundwater because of the high sulphate and calcium activities. Near saturation with respect to gypsum is predicted by SOLVEQ (Reed and Spycher, 1989) for the more sulphate contaminated samples. Indeed, recent gypsum precipitation has been documented using XRD on soil samples taken from 15 cm to 200 cm depth adjacent to the sulphur pads. The relative depletion of ^{18}O and relative enrichment of ^{34}S in the soluble sulphate fraction of these samples confirms that the gypsum originates from anthropogenic sulphate. In addition, the ^{34}S depletion of insoluble sulphate from soil samples taken at 60 and 90 cm depth suggests preferential incorporation of the lighter sulphur isotope into an insoluble form.

Thus, geochemical and isotope data not only has proven useful in tracing the path of anthropogenic sulphate in groundwater but has also provided information about the geochemical alterations associated with sulphate contamination of groundwater.

REFERENCES

- Abercrombie H. 1989. Water-Rock Interaction During Diagenesis and Thermal Recovery, Cold Lake, Alberta. PhD Thesis. University of Calgary. Department of Geology and Geophysics. Calgary, Alberta. Canada.
- Bayliss P. 1986. Quantitative Analysis of Sedimentary Minerals by Powder X-Ray Diffraction. Powder Diffraction. vol. 1. no.2.
- Bryant R.D., Jansen W., Boivin J., Laishley E.J., Costerton J.W. 1991. Effect of Hydrogenase and Mixed Sulfate-Reducing Bacterial Populations on the Corrosion of Steel. Applied and Environmental Microbiology. vol. 57. no.10. 2804-2809.
- Bryant R.D., Laishley E.J. 1990. The role of hydrogenase in anaerobic biocorrosion. Canadian J. of Microbiology. vol. 36.
- Brown G.W., Berman R.G., Perkins E.H. 1988. GEO-CALC: A software package for rapid calculation of stable pressure-temperature-activity phase diagrams using an IBM or compatible personal computer. Computers and Geosciences. vol. 14. 279-289.
- CCREM (Canadian Council of Resource and Environment Ministers). 1987. Canadian Water Quality Guidelines.
- Chambers L.A., Trudinger P.A. 1979. Microbiological fractionation of stable sulphur isotopes: A review and critique. Geomicrobiol. J. 249-293.
- Classen H.C. 1982. Guidelines and Techniques for Obtaining Water Samples That Accurately Represent the Water Chemistry of an Aquifer. USGS open file rpt #82-1024
- Coleman M.C., Sheperd T.J., Durham J.J., Rouse J.D., Moore G.R. 1982. Reduction of water with zinc for hydrogen isotope analysis. Anal. Chem. vol. 54. 993-995.
- Costerton J.W., Boivin J.W., Laishley E.J., Bryant R.D., 1989. A New Test For Microbial Corrosion. In: Proceedings of the 6th Annual Asian-Pacific Corrosion Control Conference.
- Craig H. 1961a. Isotopic variations in meteoric waters. Science 133. 1702.
- Craig H. 1961b. Standard for reporting concentration of deuterium and oxygen-18. Science 133. 1833.

- Domenico P.A., Schwartz F.W.. 1990. Physical and Chemical Hydrogeology. John Wiley & Sons. 465-468
- Dowuona G.N., Mermut A.R., Krouse H.R. 1993. Stable isotope geochemistry of sulphate in relation to hydrogeology in southern Saskatchewan, Canada. Applied Geochemistry. vol. 8. 255-263.
- Drever J.I. 1988. The Geochemistry of Natural Waters 2nd ED. Prentice-Hall Inc. Toronto.
- Epstein S., Mayeda T.K. 1953. Variation of ¹⁸O content of waters from natural sources. Geochim.Gosmochim Acta. vol. 4. 213-224.
- Fontes J.Ch. 1980. Environmental isotopes in hydrology, chp.3. In: P.Fritz, J.Ch. Fontes (Eds.). Handbook of Environmental Isotope Geochemistry. vol. I. Elsevier. New York. 75-140.
- Freeze R.A., Cherry J.A..1979. Groundwater. Prentice-Hall Inc. Toronto.
- Germonov A.E., Volkov G.A., Lisitsin A.K., Serebrennirov V.S. 1959. Investigation of the oxidation-reduction potential of groundwaters. Geochemistry. vol. 3, 322-329.
- HBT AGRA Limited. 1993. file no. BXO 3578. Lethbridge, Alberta.
- Hendry M.J., Cherry J.A., Wallick. 1986. Origin and Distribution of Sulfate in Fractured Till in Southern Alberta, Canada. Water Resources Research. vol. 22. 45-61.
- Hendry M.J., Krouse H.R., Shakur M.A. 1989. Interpretation of Oxygen and Sulphur Isotopes From Dissolved Sulfates in Tills of Southern Alberta, Canada. Water Resources Research. vol. 25. 567-572.
- Hitchon B., Krouse H.R. 1972. Hydrogeochemistry of the surface waters of the Mackenzie River drainage basin, Canada: III. Stable isotopes of oxygen, carbon and sulphur. Geochim.Cosmoch.Acta. vol. 36. 1337-1357.
- Hoefs J. 1973. Stable Isotope Geochemistry. Springer-Verlag. New York.
- Holowaychuk N., Fessenden R.J..1986. Soil Sensitivity to Acidic Inputs, Alberta. Alberta Research Council. Earth Science Report #87.1.

- Gat J.R., Gonfiantini R (Eds). 1981. Stable Isotope Hydrology: D and ^{18}O in the Water Cycle. IAEA. Vienna, Tech. Rp. Ser., no.210. 339
- Jeffries M.O., Krouse H.R., Shakur M.A., Harris S.A. 1984. Isotope geochemistry of stratified Lake "A", Ellesmere Island, N.W.T., Canada. *Can. J. Earth Sci.* vol. 21. 1008-1017.
- KOMEX INTERNATIONAL. 1991. file no. A91-2330-4. Calgary, Alberta. Canada.
- Krouse H.R. 1989. Case Studies and Potential Applications. In: H.R. Krouse, V.A. Grinenko (Eds). STABLE ISOTOPES Natural and Anthropogenic Sulphur in the Environment. John Wiley & Sons. Toronto, Canada.
- Krouse H.R. 1989. Sulphur Isotope Studies of the Pedosphere and Biosphere. In: P.W. Rundel, J.R. Ehleringer, K.A.Nagy (Eds). Stable Isotopes in Ecological Research. Springer-Verlag. New York.
- Krouse H.R. et al. 1989. Pedosphere and Biosphere. In: H.R. Krouse, V.A. Grinenko (Eds). STABLE ISOTOPES Natural and Anthropogenic sulphur in the Environment. John Wiley & Sons. Toronto, Canada.
- Krouse H.R., Viau C.A., Eliuk L.S., Ueda A., Halas S. 1987. Chemical and isotopic evidence of thermochemical sulphate reduction by light hydrocarbon gases in deep carbonate reservoirs. *Nature*. vol. 333. 415-419.
- Krouse H.R. 1987b. Relationships between the sulphur and oxygen isotope composition of dissolved sulphate. In: Studies on Sulphur Isotope Variations in Nature. IAEA proceedings of an advisory group meeting on the hydrology and geochemistry of sulphur isotopes organized by the International Atomic Energy Agency (IAEA) Austria June 17 to 20, 1985. 19.
- Krouse H.R., Tabatabai M.A. 1986. Stable Sulphur Isotopes. In: M.A. Tabatabai (Ed.). Sulfur in Agriculture. no.27. in the series AGRONOMY. Am.Soc. of Agronomy Inc., Crop Sci. Soc. of America Inc., Soil Sci. Soc. of America Inc. Madison, Wisconsin. USA.
- Krouse H.R. 1980. Sulphur Isotopes in Our Environment. In: P. Fritz, J.Ch. Fontes (Eds) Handbook of Environmental Isotope Geochemistry. Vol I. The Terrestrial Environment. Elsevier, New York. 435-72.

- Krouse H.R., Case J.W. 1983. Sulphur isotope abundances in the environment and their relation to long term sour gas flaring near Valleyview, Alberta. RMD Report 83/18 to Research Management and Pollution Control Divisions of Alberta Environment. Canada.
- Krouse H.R., Case J.W. 1981. Sulphur isotope ratios in water, air, soil and vegetation near Teepee Creek Gas Plant, Alberta. Water, Air and Soil Pollution.
- Krouse H.R. 1977. Sulphur isotope abundance elucidate uptake of atmospheric sulphur emissions by vegetation. NATURE. vol. 265. 45-46
- Krouse H.R. 1976. Sulphur isotope variations in thermal and mineral waters. Proceedings of International Symposium on Water-Rock Interaction. IAGC. Prague. 1974. 340-347.
- Lawrence J.R., Taylor H.P.Jr. 1971. Deuterium and oxygen-18 correlation: Clay minerals and hydroxides in Quaternary soils compared to meteoric waters. Geochim. Cosmochim. Acta. vol. 35. 993
- Leone G, Ricchiuto T.E., Longinelli A. 1987. Isotopic composition of dissolved oceanic sulphate. In: Studies on Sulphur Isotope Variations in Nature. IAEA proceedings of an advisory group meeting on the hydrology and geochemistry of sulphur isotopes organized by the International Atomic Energy Agency (IAEA) Austria June 17 to 20, 1985. 19.
- Lloyd R.M. 1967. Oxygen-18 composition of oceanic sulphate. Science 156. 1228-1231.
- Lowe L.E., Sasaki A., Krouse H.R..1971. Variations of Sulphur-34: Sulphur-32 Ratios in Soil Fractions in Western Canada. Can. J. Soil Sci. vol. 51. 129-131.
- Material Data Inc. 1993. "JADE" XRD Pattern Processing for the PC. box 791. Livermore, Ca.
- Mayer B. 1993. Untersuchungen zure Isotopengeochemie des Schwefel in Waldboden und neu gebildetem Grundwasser unter Wald. PhD Thesis. GSF-Forschungszentrum. Herausgeber.
- McCready R.G.L., Krouse H.R. 1982. Sulphur isotope fractionation during the oxidation of elemental sulphur by thiobacilli in a solonetzic soil. Can. J. Soil Sci. vol. 62, 105-110.

- Norman Ann-Lise. 1991. Stable Isotope Studies of Atmospheric Sulphur: Comparison of Alberta, Canada and Bermuda. M.Sc. Thesis. Department of Physics and Astronomy, University of Calgary. Calgary, Alberta, Canada. 162
- Nriagu J.O., Coker R.D. 1983. Sulphur in Sediments Chronicles Past Changes in Lake Acidification. NATURE. 303. 692-684.
- Parks Canada. 1987-1991. Waterton Lakes National Parks precipitation data.
- Rafter T.A., Mizutani Y. 1967. Oxygen isotopic composition of sulphates-Part2. Preliminary results on oxygen isotopic variations in sulphates and the relationship to their environment and to their $\delta^{34}\text{S}$ values. New Zealand J. Sci. vol. 10. 816-840.
- Rao S.S., Dickman M.D., Thode H.G. 1989. Isotopic and Diatom Evidence of Bacterial Sulphate Reduction in Sediments. Water Poll. Res. J. Canada. vol. 24. 215-232.
- Rees C.E. 1973. A steady-state model for sulphur isotope fractionation in bacterial reduction processes. Geochim. Cosmochim. Acta. vol. 37. 1141-1162.
- Robertson W.D., Cherry J.A., Schiff S.L. 1989. Atmospheric Sulphur Deposition 1950-1985 Inferred From Sulfate in Groundwater. Water Resources Research. vol. 25. 1111-1123.
- Shakur A. 1982. ^{34}S and ^{18}O variations in terrestrial sulphates. PhD. Thesis. Department of Physics and Astronomy, University of Calgary. Calgary Alberta, Canada. 51.
- Simpson G. 1992. Early Diagenesis in the Fraser River Delta. M.Sc. Thesis. Department of Geology and Geophysics, University of Calgary, Calgary, Alberta, Canada. 66
- Smejkal V., Cook F.D., Krouse H.R. 1971. Studies of Sulphur and Carbon Isotope Fractionation with Microorganisms Isolated from Springs of Western Canada. Geochim. Cosmochim. Acta. vol. 35. 787.
- Spycher N.F., Reed M.H. 1989. SOLVEQ: a computer program for computing Aqueous-Mineral-Gas Equilibria. Department of Geological Sciences. University of Oregon. Eugene, Oregon. 97403.

- Stalker Macs.A., Harrison J.E. 1977. Quaternary Glaciation of the Waterton-Castle River Region of Alberta. *Bull.Can.Petr.Geol.* vol.25. no.4. p882-902.
- Staniazek P. 1992. Stable Isotope Composition of Dissolved Sulphate and Carbonate in Selected Natural Systems. PhD Thesis. Department of Physics and Astronomy. University of Calgary. Calgary, Alberta. Canada.
- Tokarsky O. 1974. Hydrogeology of the Lethbridge-Fernie Area. Alberta Research Council. report #74-1.
- Twin Butte Soils and Water Evaluation Task Force. 1984. Appendices Relative to Hydrology. vol. II, Appendix H-I. Province of Alberta, Canada.
- Trembaczowski A. 1991. Sulphur and Oxygen Isotopes Behaviour in Sulphates of Atmospheric Groundwater System Observations and Model. *Nordic Hydrology.* vol. 22. 49-66.
- Ueda A., Krouse H.R. 1986. Direct conversion of sulphide and sulphate minerals to SO₂ for isotope analysis. *Geochem.J.* #20. 209-212
- van Donkelaar C, Hutcheon I.E., Krouse H.R.. 1992. Sulphur and Oxygen Isotope Abundances in Groundwater Sulphate Near a Sour Gas Plant. In: *Proceedings: Sulphur Transformations in Soil Ecosystems.* National Hydrology Research Institute. Saskatoon, Canada. 245.
- van Donkelaar C. 1991. Sulphate $\delta^{34}\text{S}$ in vegetation, soil and water at Jumping Pound Sour Gas Plant. unpublished report.
- van Stempvoort D.R., Reardon E.J., Fritz P. 1990. Fractionation of sulphur and oxygen isotopes in sulfate by soil sorption. *Geochim. Cosmochim. Acta.* vol. 54. 2817-2826.
- Yanagisawa F., Sakai H. 1983. Thermal decomposition of barium sulphate-vanadium pentoxide-silica mixtures for the preparation of sulphur dioxide in sulphur isotope ratio measurement. *Analyt. Chem.* vol. 55. 985-987.
- Yonge C.J., Goldenberg L., H.R.Krouse. 1989. An isotope study of water bodies along a traverse of southwestern Canada. *J. Hydrol.* vol. 106. 245-255.